



Aqueous secondary organic aerosol formation from the direct photosensitized oxidation of vanillin in the absence and presence of ammonium nitrate

Brix Raphael Go^{1,2}, Yan Lyu^{1,2}, Yan Ji^{1,2}, Yong Jie Li³, Dan Dan Huang⁴, Xue Li⁵, Theodora Nah¹, Chun Ho Lam¹, and Chak K. Chan^{1,2,6}

¹School of Energy and Environment, City University of Hong Kong, Kowloon, Hong Kong, China

²City University of Hong Kong Shenzhen Research Institute, Shenzhen, China

³Department of Civil and Environmental Engineering, and Centre for Regional Oceans, Faculty of Science and Technology, University of Macau, Taipa, Macau 999078, China

⁴State Environmental Protection Key Laboratory of Formation and Prevention of the Urban Air Pollution Complex, Shanghai Academy of Environmental Sciences, Shanghai 200233, China

⁵Institute of Mass Spectrometry and Atmospheric Environment, Jinan University, No. 601 Huangpu Avenue West, Guangzhou 510632, China

⁶Guy Carpenter Asia-Pacific Climate Impact Center, City University of Hong Kong, Kowloon, Hong Kong, China

Correspondence: Chak K. Chan (chak.k.chan@cityu.edu.hk)

Received: 11 May 2021 – Discussion started: 17 May 2021

Revised: 2 December 2021 – Accepted: 2 December 2021 – Published: 10 January 2022

Abstract. Vanillin (VL), a phenolic aromatic carbonyl abundant in biomass burning emissions, forms triplet excited states ($^3\text{VL}^*$) under simulated sunlight leading to aqueous secondary organic aerosol (aqSOA) formation. Nitrate and ammonium are among the main components of biomass burning aerosols and cloud or fog water. Under atmospherically relevant cloud and fog conditions, solutions composed of either VL only or VL with ammonium nitrate were subjected to simulated sunlight irradiation to compare aqSOA formation via the direct photosensitized oxidation of VL in the absence and presence of ammonium nitrate. The reactions were characterized by examining the VL decay kinetics, product compositions, and light absorbance changes. Both conditions generated oligomers, functionalized monomers, and oxygenated ring-opening products, and ammonium nitrate promoted functionalization and nitration, likely due to its photolysis products ($^{\bullet}\text{OH}$, $^{\bullet}\text{NO}_2$, and NO_2^- or HONO). Moreover, a potential imidazole derivative observed in the presence of ammonium nitrate suggested that ammonium participated in the reactions. The majority of the most abundant products from both conditions were potential brown carbon (BrC) chromophores. The effects of oxygen (O_2), pH, and reactants concentration and molar ratios on the reactions were also explored. Our findings show that O_2 plays an essential role in the reactions, and oligomer formation was enhanced at $\text{pH} < 4$. Also, functionalization was dominant at low VL concentrations, whereas oligomerization was favored at high VL concentrations. Furthermore, oligomers and hydroxylated products were detected from the oxidation of guaiacol (a non-carbonyl phenol) via VL photosensitized reactions. Last, potential aqSOA formation pathways via the direct photosensitized oxidation of VL in the absence and presence of ammonium nitrate were proposed. This study indicates that the direct photosensitized oxidation of VL may be an important aqSOA source in areas influenced by biomass burning and underscores the importance of nitrate in the aqueous-phase processing of aromatic carbonyls.

1 Introduction

Aqueous reactions can be an important source of secondary organic aerosols (SOAs; Blando and Turpin, 2000; Volkamer et al., 2009; Lim et al., 2010; Ervens et al., 2011; Huang et al., 2011; Lee et al., 2011; Smith et al., 2014), such as highly oxygenated and low-volatility organics (Hoffmann et al., 2018; Liu et al., 2019), which may affect aerosol optical properties due to contributions to brown carbon (BrC; Giarlioni et al., 2016). BrC refers to organic aerosols that absorb radiation efficiently in the near-ultraviolet (UV) and visible regions (Laskin et al., 2015). The formation of aqueous SOA (aqSOA) via photochemical reactions involves oxidation, with the hydroxyl radical ($\cdot\text{OH}$) usually considered as being the primary oxidant (Herrmann et al., 2010; Smith et al., 2014). The significance of photosensitized chemistry in atmospheric aerosols has recently been reviewed (George et al., 2015). For instance, triplet excited states of organic compounds ($^3\text{C}^*$) from the irradiation of light-absorbing organics such as non-phenolic aromatic carbonyls (Canonica et al., 1995; Anastasio et al., 1997; Vione et al., 2006; Smith et al., 2014) have been reported to oxidize phenols at higher rates and with greater aqSOA yields compared to $\cdot\text{OH}$ (Sun et al., 2010; Smith et al., 2014; Yu et al., 2014; Smith et al., 2016). Aside from being an oxidant, $^3\text{C}^*$ can also be a precursor of singlet oxygen ($^1\text{O}_2$), superoxide ($\text{O}_2^{\cdot-}$) or hydroperoxyl ($\cdot\text{HO}_2$) radicals, and $\cdot\text{OH}$ (via $\text{HO}_2^{\cdot}/\text{O}_2^{\cdot-}$ formation) upon reactions with O_2 and substrates (e.g., phenols; George et al., 2018). The $^3\text{C}^*$ concentration in typical fog water has been estimated to be >25 times than that of $\cdot\text{OH}$, making $^3\text{C}^*$ the primary photo-oxidant for biomass burning phenolic compounds (Kaur and Anastasio, 2018; Kaur et al., 2019). Recent works on triplet-driven oxidation of phenols have mainly focused on changes in physicochemical properties (e.g., light absorption) and aqSOA yield (e.g., Smith et al., 2014, 2015, 2016), with few reports on reaction pathways and products (e.g., Yu et al., 2014; Chen et al., 2020; Jiang et al., 2021).

Inorganic salts such as ammonium nitrate are major components of aerosols and cloud or fog water. In cloud and fog water, the concentrations of inorganic nitrate can vary from 50 to $>1000\ \mu\text{M}$, with higher levels typically noted under polluted conditions (Munger et al., 1983; Collett et al., 1998; Zhang and Anastasio, 2003; Li et al., 2011; Giulianelli et al., 2014; Bianco et al., 2020). Upon photolysis (Vione et al., 2006; Herrmann, 2007; Scharko et al., 2014), inorganic nitrate in cloud and fog water can contribute to BrC (Minero et al., 2007) and aqSOA formation (Huang et al., 2018; Klodt et al., 2019; Zhang et al., 2021) by generating $\cdot\text{OH}$ and $\cdot\text{NO}_2$ (also a nitrating agent). For example, the aqSOA yields from the photo-oxidation of phenolic carbonyls in ammonium nitrate are twice as high as that in ammonium sulfate solution (Huang et al., 2018). Nitration is a significant process in the formation of light-absorbing organics or BrC in the atmosphere (Jacobson, 1999; Kahnt et al., 2013; Mohr et al., 2013; Laskin et al., 2015; Teich et al., 2017; Li et al., 2020).

Moreover, nitrate photolysis has been proposed to be a potentially important process for SO_2 oxidation and SOA formation via the generation of $\cdot\text{OH}$, $\cdot\text{NO}_2$, and N(III) within particles (Gen et al., 2019a, b; Zhang et al., 2020, 2021, 2022), and it can also potentially change the morphology of atmospheric viscous particles (Liang et al., 2021). Furthermore, ammonium (NH_4^+) can react with carbonyls, producing light-absorbing compounds and highly oxygenated oligomers, and catalyze different reactions (De Haan et al., 2009, 2011; Nozière et al., 2009, 2010, 2018; Shapiro et al., 2009; Yu et al., 2011; Lee et al., 2013; Powelson et al., 2014; Gen et al., 2018; Mabato et al., 2019). Therefore, $^3\text{C}^*$ and inorganic nitrate can contribute to aqSOA and BrC formation.

Biomass burning (BB) is a significant atmospheric source of both phenolic and non-phenolic aromatic carbonyls (Rogge et al., 1998; Nolte et al., 2001; Schauer et al., 2001; Bond et al., 2004). Upon exposure to sunlight, aromatic carbonyls are excited to their triplet excited states, which can initiate oxidation leading to aqSOA formation (e.g., Smith et al., 2014; 2015, 2016). An example is vanillin (VL; Henry's law constant of $4.56 \times 10^5\ \text{M atm}^{-1}$; Yaws, 1994), a phenolic aromatic carbonyl that has been used as a model compound for methoxyphenols, which are abundant in BB emissions (Li et al., 2014; Pang et al., 2019a). The aqueous $\cdot\text{OH}$ oxidation and direct photodegradation of VL have been shown to yield low-volatility products, although these findings were based on 254 nm irradiation (Li et al., 2014). Photodegradation kinetics and aqSOA yields have been reported for direct VL photodegradation under simulated sunlight (Smith et al., 2016), with oxygenated aliphatic-like compounds (high H:C, ≥ 1.5 and low O:C, ≤ 0.5 ratios) noted as being the most likely products (Loisel et al., 2021). Additionally, aqueous-phase reactions of phenols with reactive nitrogen species have been proposed to be a significant source of nitrophenols and SOA (Grosjean, 1985; Kitanovski et al., 2014; Kroflič et al., 2015, 2021; Pang et al., 2019a; Yang et al., 2021). For instance, nitrite-mediated VL photo-oxidation can generate nitrophenols, and the reactions are influenced by nitrite/VL molar ratios, pH, and the presence of $\cdot\text{OH}$ scavengers (Pang et al., 2019a). Nitrate and ammonium are also among the main biomass burning aerosol components (Xiao et al., 2020; Zielinski et al., 2020). As BB aerosols are typically internally mixed with other aerosol components (Zielinski et al., 2020), VL may coexist with ammonium nitrate in BB aerosols. The direct photosensitized oxidation of VL in the absence and presence of ammonium nitrate may then reveal insights into the atmospheric processing of BB aerosols. Moreover, the $^3\text{C}^*$ of non-phenolic aromatic carbonyls (e.g., 3,4-dimethoxybenzaldehyde – DMB; a non-phenolic aromatic carbonyl; Smith et al., 2014; Yu et al., 2014; Jiang et al., 2021) and phenolic aromatic carbonyls (e.g., acetosyringone and VL; Smith et al., 2016) have been shown to oxidize phenols, but the reaction products from the latter are unknown.

Previous works on aqSOA formation via triplet-mediated oxidation are mostly based on reactions between phenols and a non-phenolic aromatic carbonyl as triplet precursor (e.g., Smith et al., 2014; Yu et al., 2014; Jiang et al., 2021). Also, studies examining the effects of inorganic nitrate on aqSOA formation and properties remain limited. The present study aimed to evaluate aqSOA formation via the direct photosensitized oxidation of a triplet precursor (VL) alone. Furthermore, aqSOA formation via the direct photosensitized oxidation of VL in the presence of ammonium nitrate was also examined. Accordingly, the main goals of this study are (1) to compare aqSOA formation in cloud and fog water via the direct photosensitized oxidation of VL in the absence and presence of ammonium nitrate; (2) to evaluate the influences of O₂, solution pH, and reactants concentration and molar ratios on the reactions; (3) to investigate the participation of ammonium in the direct photosensitized oxidation of VL in the presence of ammonium nitrate; and (4) to examine aqSOA formation from the oxidation of guaiacol, a non-carbonyl phenol, via photosensitized reactions of VL. To achieve these goals, solutions composed of either VL only or VL in the presence of ammonium nitrate were subjected to simulated sunlight irradiation under atmospherically relevant cloud and fog conditions. Solutions composed of VL in the presence of sodium nitrate were also examined for comparison with the presence of ammonium nitrate. The reactions were characterized based on VL decay kinetics, detected products, and light absorbance changes. Finally, we proposed aqSOA formation pathways via the direct photosensitized oxidation of VL in the absence and presence of ammonium nitrate. This work presents a comprehensive comparison of aqSOA formation from the direct photosensitized oxidation of VL in the absence and presence of ammonium nitrate.

2 Methods

2.1 Aqueous-phase photo-oxidation experiments

Photo-oxidation experiments were performed in a custom-built quartz photo reactor. The solutions (initial volume of 500 mL) were continuously mixed throughout the experiments using a magnetic stirrer. The solutions were bubbled with synthetic air or nitrogen (N₂; > 99.995 %; 0.5 dm³/min) for 30 min before irradiation to achieve air- or N₂-saturated conditions, respectively, and the bubbling was continued throughout the reactions (Du et al., 2011; Chen et al., 2020). The aim of the air-saturated experiments was to enable the generation of secondary oxidants (¹O₂, O₂^{•−} / [•]HO₂, and [•]OH) from ³VL* as O₂ is present. Conversely, the N₂-saturated experiments would inhibit the formation of these secondary oxidants, which can lead to ³VL*-driven reactions (Chen et al., 2020). Comparison of results of air- and N₂-saturated experiments can yield information on the reaction pathways that require O₂ involved in the direct photosensitized oxidation of VL. In this study, the reactions can

generate ³VL* and secondary oxidants (¹O₂, O₂^{•−} / [•]HO₂, and [•]OH) but not ozone; hence, we focused on reactions involving the former. Solutions were irradiated through the quartz window of the reactor using a xenon lamp (model 6258; ozone-free xenon lamp; 300 W; Newport) equipped with a longpass filter (20CGA 305 nm cut-on filter; Newport) to eliminate light below 300 nm. Cooling fans positioned around the photo reactor and lamp housing maintained reaction temperatures at 27 ± 2 °C. The averaged initial photon flux in the reactor from 300 to 380 nm, measured using a chemical actinometer (2-nitrobenzaldehyde), was 2.6 × 10¹⁵ photons cm^{−2} s^{−1} nm^{−1} (Fig. S1). Although the concentration of VL in cloud or fog water has been estimated to be <0.01 mM (Anastasio et al., 1997), a higher VL concentration (0.1 mM) was used in this study to guarantee sufficient signals for product identification (Vione et al., 2019). The chosen ammonium nitrate (AN) or sodium nitrate (SN) concentration (1 mM) was based on values observed in cloud and fog water (Munger et al., 1983; Collett et al., 1998; Zhang and Anastasio, 2003; Li et al., 2011; Giulianelli et al., 2014; Bianco et al., 2020). It should be noted that this study is not intending to identify the concentrations of ammonium nitrate that would affect the kinetics but to examine the effect of ammonium nitrate on aqSOA formation from the direct photosensitized oxidation of VL. Moreover, the photo-oxidation of guaiacol (GUA; 0.1 mM), a non-carbonyl phenol, in the presence of VL (0.1 mM) was studied. The GUA experiments allowed us to examine aqSOA formation from the oxidation of phenols by ³VL*. Samples (10 mL) were collected hourly for a total of 6 h for offline chemical and optical analyses. VL (and GUA) decay kinetics measurements (calibration curves for VL and GUA standard solutions; Fig. S2), product characterization, small organic acids measurements, and absorbance measurements were conducted using ultra-high-performance liquid chromatography (UHPLC) with a photodiode array detector (UHPLC-PDA), a UHPLC coupled with quadrupole time-of-flight mass spectrometry (UHPLC-qToF-MS) equipped with an electrospray ionization (ESI) source and operated in the positive ion mode (the negative ion mode signals were too low for our analyses), ion chromatography (IC), and UV-Vis spectrophotometry, respectively. Each experiment was repeated independently at least 3 times, and measurements were done in triplicate. The reported decay rate constants and absorbance enhancement are the average of the results from triplicate experiments, and the corresponding errors represent 1 standard deviation. The mass spectra are based on the average of results from duplicate experiments. The Supplement (Sects. S1 to S6) provides details on the materials and analytical procedures. The pseudo-first-order rate constant (*k'*) for VL decay was determined using the following equation (Huang et al., 2018):

$$\ln([\text{VL}]_t/[\text{VL}]_0) = -k't, \quad (1)$$

where $[\text{VL}]_t$ and $[\text{VL}]_0$ are the concentrations of VL at time t and 0, respectively. Replacing VL with GUA in Eq. (1) enabled the calculation of the GUA decay rate constant. The decay rate constants were normalized to the photon flux measured for each experiment through dividing k' by the measured 2-nitrobenzaldehyde (2NB) decay rate constant, $j(2\text{NB})$ (see Sect. S6 for more details).

2.2 Calculation of normalized abundance of products

Comparisons of peak abundance in mass spectrometry have been used in many recent studies (e.g., Lee et al., 2014; Romonosky et al., 2017; Wang et al., 2017; Fleming et al., 2018; Song et al., 2018; Klodt et al., 2019; Ning et al., 2019) to show the relative importance of different types of compounds (Wang et al., 2021). However, ionization efficiency may greatly vary for different classes of compounds (Kearle, 2000; Schmidt et al., 2006; Leito et al., 2008; Perry et al., 2008; Krueve et al., 2014), and so uncertainties may arise from comparisons of peak areas among compounds. In this work, we assumed equal ionization efficiency of different compounds, which is commonly used to estimate O:C ratios of SOA (e.g., Bateman et al., 2012; Lin et al., 2012; Laskin et al., 2014; De Haan et al., 2019) to calculate their normalized abundance. The normalized abundance of a product, $[\text{P}]$ (unitless), was calculated as follows:

$$[\text{P}] = \frac{A_{\text{P},t}}{A_{\text{VL},t}} \cdot \frac{[\text{VL}]_t}{[\text{VL}]_0}, \quad (2)$$

where $A_{\text{P},t}$ and $A_{\text{VL},t}$ are the extracted ion chromatogram (EIC) peak areas of the product P and VL from UHPLC-qToF-MS analyses at time t , respectively. $[\text{VL}]_t$ and $[\text{VL}]_0$ are the VL concentrations (μM) determined using UHPLC-PDA at time t and 0, respectively. Here, we relied on the direct quantification of [VL] using UHPLC-PDA (see Fig. S2 for the VL calibration curve). We emphasize that the normalized abundance of products in this study is a semi-quantitative analysis intended to provide an overview of how the signal intensities changed under different experimental conditions but not to quantify the absolute concentration of products. Also, as it is based on comparisons of peak abundance from UHPLC-qToF-MS analyses, the normalized abundance of products in this study is associated with intrinsic uncertainties due to the variability in ionization efficiencies for various compounds. Moreover, the major products detected in this study are probably those with high concentration or high ionization efficiency in the positive ESI mode. The use of relative abundance (product peaks are normalized to the highest peak; e.g., Lee et al., 2014; Romonosky et al., 2017; Fleming et al., 2018; Klodt et al., 2019) would yield the same major products reported. Typical fragmentation behavior observed in MS/MS spectra for individual functional groups from Holčápek et al. (2010) are outlined in Table S1.

3 Results and discussion

3.1 Kinetics, mass spectrometric, and absorbance changes analyses during the direct photosensitized oxidation of VL in the aqueous phase

For clarity purposes, the reactions involving reactive species referred to in the following discussions are provided in Table 1. Table 2 summarizes the reaction conditions, initial VL (and GUA) decay rate constants, normalized abundance of products, and average carbon oxidation state ($\langle\text{OS}_\text{C}\rangle$) of the 50 most abundant products. In general, the 50 most abundant products contributed more than half of the total normalized abundance of products and can facilitate the discussions of reaction pathways and calculation of the $\langle\text{OS}_\text{C}\rangle$.

As shown in Fig. S3, VL underwent oxidation both directly and in the presence of ammonium (and sodium) nitrate upon simulated sunlight illumination. VL absorbs light and is promoted to its excited singlet state ($^1\text{VL}^*$) and then undergoes inter-system crossing (ISC) to the excited triplet state, $^3\text{VL}^*$. In principle, $^3\text{VL}^*$ can oxidize ground-state VL (type I photosensitized reactions) via H atom abstraction or electron transfer, and form $\text{O}_2^{\bullet-}$ or HO_2^{\bullet} in the presence of O_2 (George et al., 2018), or react with O_2 (type II photosensitized reactions) to yield $^1\text{O}_2$ via energy transfer or $\text{O}_2^{\bullet-}$ via electron transfer (Lee et al., 1987; Foote et al., 1991). The disproportionation of $\text{HO}_2^{\bullet} / \text{O}_2^{\bullet-}$ (Anastasio et al., 1997) form hydrogen peroxide (H_2O_2), which is a photolytic source of $\bullet\text{OH}$. Overall, air-saturated conditions, in which O_2 is present, enable the generation of secondary oxidants ($^1\text{O}_2$, $\text{O}_2^{\bullet-} / \bullet\text{HO}_2$, and $\bullet\text{OH}$) from $^3\text{VL}^*$. However, as discussed later, we found that the direct photosensitized oxidation of VL under air-saturated conditions in this study is mainly governed by $^3\text{VL}^*$. Moreover, $\bullet\text{OH}$, $\bullet\text{NO}_2$, and $\text{NO}_2^- / \text{HNO}_2$, i.e., N(III), generated via nitrate photolysis (Reactions 1–3; Table 1), can also oxidize or nitrate VL. In this work, the direct photosensitized oxidation of VL in the absence (VL-only experiments) and presence of ammonium nitrate are referred to as VL* and VL + AN, respectively.

3.1.1 VL photo-oxidation under N_2 and air-saturated conditions

As previously stated, the air-saturated experiments can enable the generation of secondary oxidants ($^1\text{O}_2$, $\text{O}_2^{\bullet-} / \bullet\text{HO}_2$, and $\bullet\text{OH}$) from $^3\text{VL}^*$ as O_2 is present. In contrast, the N_2 -saturated experiments would inhibit the formation of these secondary oxidants from $^3\text{VL}^*$, facilitating $^3\text{VL}^*$ -driven reactions (Chen et al., 2020). Moreover, Chen et al. (2020) reported that, for experiments conducted under three saturated gases (air, O_2 , and N_2), the rate constant for 4-ethylguaicol (a non-carbonyl phenol) loss by $^3\text{DMB}^*$ decreased in the order of air > N_2 > O_2 . The higher rate constant under N_2 -saturated conditions compared to that under O_2 -saturated conditions indicates that $^3\text{DMB}^*$ is a more important con-

Table 1. List of reactions involving reactive species relevant to this study.

No.	Reactions	References
1	$\text{NO}_3^- + \text{h}\nu \rightarrow \bullet\text{NO}_2 + \text{O}^-; \phi = 0.01$	Vione et al. (2006); Benedict et al. (2017)
2	$\text{O}^- + \text{H}_3\text{O}^+ \leftrightarrow \bullet\text{OH} + \text{H}_2\text{O}$	
3	$\text{NO}_3^- + \text{h}\nu \rightarrow \text{NO}_2^- + \text{O}(\text{}^3\text{P}); \phi = 0.011$	
4	$\text{NO}_2^- + \bullet\text{OH} \rightarrow \bullet\text{NO}_2 + \text{OH}^- (k = 1.0 \times 10^{10} \text{ M}^{-1} \text{ s}^{-1})$	Mack and Bolton (1999); Pang et al. (2019a)
5	$\text{O}_2^{\bullet-} + \text{NO}_2^- + 2\text{H}^+ \rightarrow \bullet\text{NO}_2 + \text{H}_2\text{O}_2$	Vione et al. (2001); Pang et al. (2019a)
6	$\text{NO}_2^- + \text{h}\nu \rightarrow \bullet\text{NO} + \text{O}^-; \phi_{\text{OH}, 300} = 6.7(\pm 0.9)\%$	Fischer and Warneck (1996); Mack and Bolton (1999); Pang et al. (2019a)
7	$\bullet\text{NO} + \text{O}_2 \leftrightarrow \bullet\text{ONOO}$	Goldstein and Czapski (1995);
8	$\bullet\text{ONOO} + \bullet\text{NO} \rightarrow \text{ONOONO}$	Pang et al. (2019a)
9	$\text{ONOONO} \rightarrow 2\bullet\text{NO}_2$	
10	$\text{HNO}_2 + \bullet\text{OH} \rightarrow \bullet\text{NO}_2 + \text{H}_2\text{O} (k = 2.6 \times 10^9 \text{ M}^{-1} \text{ s}^{-1})$	Kim et al. (2014); Pang et al. (2019a)

tributor than $^1\text{O}_2$ for 4-ethylguaiacol degradation. The highest rate constant noted under air-saturated conditions was attributed to the presence of O_2 , resulting in a synergistic effect of $^1\text{O}_2$ and $^3\text{C}^*$. The differences in air-saturated and N_2 -saturated experiments can then be used to infer the role of reaction pathways that require O_2 in the direct photosensitized oxidation of VL. The photosensitized oxidation of VL under both N_2 - and air-saturated conditions (Fig. S3a) were carried out at pH 4, which is representative of moderately acidic aerosol and cloud pH values (Pye et al., 2020). No significant VL loss was observed for dark experiments. The oxidation of ground-state VL by $^3\text{VL}^*$ via H atom abstraction or electron transfer can form phenoxy (which is in resonance with a carbon-centered cyclohexadienyl radical that has a longer lifetime) and ketyl radicals (Neumann et al., 1986a, b; Anastasio et al., 1997). The coupling of phenoxy radicals or phenoxy and cyclohexadienyl radicals can form oligomers, as observed for both air-saturated and N_2 -saturated experiments (see discussions later). The VL decay rate constant for VL^* under air-saturated conditions was 4 times higher than under N_2 -saturated conditions (Table 2). As mentioned earlier, secondary oxidants ($^1\text{O}_2$, $\text{O}_2^{\bullet-}$ / $\bullet\text{HO}_2$, and $\bullet\text{OH}$) can be generated from $^3\text{VL}^*$ when O_2 is present (under air-saturated conditions). However, the direct photosensitized oxidation of VL in this study is likely governed by $^3\text{VL}^*$, and these secondary oxidants have only minor participation. For instance, $^1\text{O}_2$ is also a potential oxidant for phenols (Herrmann et al., 2010; Minella et al., 2011; Smith et al., 2014), but $^1\text{O}_2$ reacts much faster (by ~ 60 times) with phenolate ions than neutral phenols (Tratnyek and Hoigne, 1991; Canonica et al., 1995; McNally et al., 2005). Under the pH values (pH 2.5 to 4) considered in this study, the amount of phenolate ion is negligible ($\text{p}K_a$ of VL = 7.9), so the reaction between VL and $^1\text{O}_2$ should be slow. Interestingly, however, both $^3\text{C}^*$ and $^1\text{O}_2$ have been shown to be important in the photo-oxidation of 4-ethylguaiacol ($\text{p}K_a = 10.3$) by $^3\text{DMB}^*$ (solution with

pH of ~ 3 ; Chen et al., 2020). Furthermore, while the irradiation of other phenolic compounds can produce H_2O_2 , a precursor for $\bullet\text{OH}$ (Anastasio et al., 1997), the amount of H_2O_2 is small. Based on this, only trace amounts of H_2O_2 were likely generated from VL^* (Li et al., 2014) under air-saturated conditions, suggesting that the contribution from $\bullet\text{OH}$ was minor. Overall, these suggest that the direct photosensitized oxidation of VL in this study is mainly driven by $^3\text{VL}^*$.

Contrastingly, the minimal decay of VL under N_2 -saturated conditions can be attributed to the phenoxy (which is in resonance with a carbon-centered cyclohexadienyl radical that has a longer lifetime) and ketyl radicals formed upon oxidation of ground-state VL by $^3\text{VL}^*$ decaying via back-hydrogen transfer to regenerate VL (Lathioor et al., 1999). A possible explanation for this is the involvement of O_2 in the secondary steps of VL decay. For instance, a major fate of the ketyl radical is a reaction with O_2 (Anastasio et al., 1997). In the absence of O_2 , radical formation occurs, but the forward reaction of ketyl radical and O_2 is blocked, leading to the regeneration of VL, as suggested by the minimal VL decay. Aside from potential inhibition of secondary oxidants generation (Chen et al., 2020), N_2 purging may have also hindered the secondary steps for VL decay.

The VL decay rate constant for VL + AN under air-saturated conditions was also higher (6.6 times) than under N_2 -saturated conditions, possibly due to reactions facilitated by nitrate photolysis products that may have been enhanced in the presence of O_2 (Vione et al., 2005; Kim et al., 2014; Pang et al., 2019a). As shown later, more N-containing species were observed for VL + AN under air-saturated conditions than under N_2 -saturated conditions. An example is enhanced VL nitration likely from increased $\bullet\text{NO}_2$ formation, such as from the reaction of $\bullet\text{OH}$ and $\text{O}_2^{\bullet-}$ with NO_2^- (Reactions 4 and 5, respectively; Table 1) or the autoxidation of $\bullet\text{NO}$ from NO_2^- photolysis (Reactions 6–9; Table 1)

Table 2. Reaction conditions, initial VL (and GUA) decay rate constants, normalized abundance of products, and average carbon oxidation state ($\langle OS_c \rangle$) in each experiment. Except where noted, the reaction systems consisted of VL (0.1 mM), GUA (0.1 mM), AN (1 mM), and SN (1 mM) under air-saturated conditions after 6 h of simulated sunlight irradiation. Analyses were performed using UHPLC-qToF-MS equipped with an ESI source and operated in the positive ion mode.

Exp no.	pH	Reaction conditions	Initial VL (and GUA) decay rate constants (min^{-1}) ^b	Ratio of 50 most abundant products to total products ^c	Normalized abundance of products ^d	Normalized abundance of N-containing compounds ^d	$\langle OS_c \rangle^e$ (OS_c of VL is -0.25 ; OS_c of GUA is -0.57)
A1	2.5	VL*	$2.0 \times 10^{-2} \pm 5.8 \times 10^{-5}$	0.59	1.7 ± 0.16	NA	-0.05
A2		VL + AN	$1.7 \times 10^{-2} \pm 7.3 \times 10^{-4}$	0.63	1.4 ± 0.19	5.3×10^{-2}	-0.04
A3	3	VL*	$1.5 \times 10^{-2} \pm 4.2 \times 10^{-4}$	0.53	1.9 ± 0.33	NA	-0.04
A4		VL + AN	$1.5 \times 10^{-2} \pm 2.3 \times 10^{-4}$	0.56	1.9 ± 0.30	3.6×10^{-2}	-0.05
A5	4	VL*	$1.2 \times 10^{-2} \pm 5.9 \times 10^{-4}$	0.58	0.26 ± 0.42	NA	-0.16
A6		VL* (N ₂ saturated)	$3.2 \times 10^{-3} \pm 1.1 \times 10^{-3}$	0.96	$4.7 \times 10^{-2} \pm 0.0027$	NA	-0.24
A7		VL + AN	$1.2 \times 10^{-2} \pm 8.8 \times 10^{-4}$	0.53	0.37 ± 0.38	1.7×10^{-2}	-0.13
A8		VL + AN (N ₂ saturated)	$1.9 \times 10^{-3} \pm 9.2 \times 10^{-5}$	0.89	0.12 ± 0.0095	6.3×10^{-3}	-0.21
A9		VL + SN	$1.3 \times 10^{-2} \pm 3.5 \times 10^{-4}$	0.51	0.42 ± 0.33	1.7×10^{-2}	-0.07
A10		VL* (0.01 mM) ^a	NA	0.90	0.37 ± 0.018	NA	-0.07
A11		VL (0.01 mM) + AN (0.01 mM)	NA	0.77	0.40 ± 0.074	8.6×10^{-3}	0.12
A12		VL (0.01 mM) + AN	NA	0.42	0.45 ± 0.025	1.2×10^{-2}	-0.06
A13		GUA only	$6.2 \times 10^{-3} \pm 2.5 \times 10^{-4}$	0.77	NA	NA	-0.28
A14		GUA + VL	GUA is $1.4 \times 10^{-2} \pm 4.0 \times 10^{-4}$ VL is $4.3 \times 10^{-3} \pm 2.2 \times 10^{-4}$	0.60	2.2 ± 0.47	NA	-0.27

^a Irradiation time for VL* (0.01 mM, A10) was 3 h. ^b The data fitting was performed in the initial linear region. Each value is the average of results from triplicate experiments. Errors represent 1 standard deviation. Kinetic measurements were not performed for experiments marked with NA (not available). ^c Ratio of the normalized abundance of the 50 most abundant products to that of total products, except for direct GUA photodegradation and GUA + VL (A13 and A14), whose ratios are based on the absolute signals of products. ^d The normalized abundance of products was calculated using Eq. (2). The samples for experiments without nitrate (marked with NA) were not analyzed for N-containing compounds. For the GUA experiments, the normalized abundance of products was calculated only for GUA + VL as the GUA signal from the UHPLC-qToF-MS in the positive ion mode was weak, which may introduce large uncertainties during normalization. ^e $\langle OS_c \rangle$ of the 50 most abundant products.

in aqueous solutions (Pang et al., 2019a). Nevertheless, the comparable decay rate constants for VL* and VL + AN imply that ³VL* chemistry still dominates, even at 1 : 10 molar ratio of VL / AN. This can be attributed to the much higher molar absorptivity of VL compared to that of nitrate (Fig. S1) and the high VL concentration (0.1 mM) used in this study. The quantification of the oxidants in our reaction systems is not explored here and requires additional work. In essence, the N₂-saturated experiments suggest that the secondary steps for VL decay via ³VL* may require O₂ to proceed. Nonetheless, further study on the impact of O₂ on the reactive intermediates involved is required to understand the exact mechanisms occurring under air-saturated conditions.

The products from VL* under N₂-saturated conditions were mainly oligomers (e.g., C₁₆H₁₄O₄; Fig. 1a), consistent with triplet-mediated oxidation forming higher molecular weight products, with less fragmentation relative to oxidation by [•]OH (Yu et al., 2014; Chen et al., 2020). A three-fold increase in the normalized abundance of products was noted upon addition of AN (VL + AN under N₂-saturated conditions; Fig. 1b), and in addition to oligomers, functionalized monomers (e.g., C₈H₆O₅) and N-containing compounds (e.g., C₈H₉NO₃; no. 3 in Table S2) were also observed, which is in agreement with [•]OH-initiated oxidation yielding more functionalized/oxygenated products compared to triplet-mediated oxidation (Yu et al., 2014; Chen et al., 2020). Oligomers, functionalized monomers (e.g.,

demethylated VL; Fig. S4), and N-containing compounds (e.g., $C_{16}H_{10}N_2O_9$; no. 4 in Table S2; for VL + AN) had higher normalized abundance under air-saturated conditions (Fig. 1c, d), which are attributable to efficient $^3VL^*$ -initiated oxidation and enhanced VL nitration in the presence of O_2 . For both VL^* and VL + AN under air-saturated conditions, the most abundant product was $C_{10}H_{10}O_5$ (no. 5 in Table S2), which is a substituted VL. Irradiation of VL by a 254 nm lamp has also been reported to lead to VL dimerization and functionalization via ring-retaining pathways, as well as small oxygenates formation, but only when $\cdot OH$ from H_2O_2 were involved (Li et al., 2014). In this work, small organic acids (e.g., formic acid) were observed from both VL^* and VL + AN under air-saturated conditions (Fig. S5) due to simulated sunlight that could access the 308 nm VL band (Smith et al., 2016). Interestingly, we observed a potential imidazole derivative ($C_5H_5N_3O_2$; no. 6 in Table S2) from VL + AN under air-saturated conditions (Fig. 1d), which may have formed from reactions induced by ammonium. This compound was not observed in a parallel experiment in which AN was replaced with SN (Fig. S6a; see Sect. 3.1.3 for the discussion).

The potential aqSOA formation pathways via the direct photosensitized oxidation of VL in the absence and presence of AN in this study are summarized in Fig. 2. At pH 4, $^3VL^*$ -initiated reactions yielded oligomeric species such as $C_{16}H_{12}O_6$ and $C_{22}H_{22}O_6$. Earlier works on phenolic aqSOA formation have reported that oligomers can form via the coupling of phenoxy radicals or phenoxy and cyclohexadienyl radicals (Sun et al., 2010; Yu et al., 2014; Vione et al., 2019). In this work, phenoxy radicals (in resonance with a carbon-centered cyclohexadienyl radical) can be generated from several processes, such as the oxidation of ground-state VL by $^3VL^*$ via H atom abstraction or electron transfer coupled with proton transfer from the phenoxy radical cation or from solvent water (Neumann et al., 1986a, b; Anastasio et al., 1997) and photoinduced O–H bond breaking (Berto et al., 2016). Also, similar reactions can be initiated by $\cdot OH$ (Gelencsér et al., 2003; Hoffer et al., 2004; Chang and Thompson, 2010; Sun et al., 2010), which, in this study, can be generated from the reaction between $^3VL^*$ and O_2 , as well as nitrate photolysis. Trace amounts of H_2O_2 could be formed during VL photodegradation (Li et al., 2014), similar to the case of other phenolic compounds (Anastasio et al., 1997). In addition, ring-opening products (Fig. S5) from fragmentation in both VL^* and VL + AN may have reacted with VL or dissolved ammonia to generate $C_{10}H_{10}O_5$ (no. 5 in Table S2; Pang et al., 2019b) or a potential imidazole derivative ($C_5H_5N_3O_2$; no. 6 in Table S2), respectively. Moreover, nitrate photolysis products promoted functionalization and nitration (e.g., $C_{16}H_{10}N_2O_9$; no. 4 in Table S2).

The molecular transformation of VL upon photosensitized oxidation was examined using the van Krevelen diagrams (Fig. S7). For all experiments (A1–14; Table 2) in this study, the O:C and H:C ratios of the products were similar to

those observed from the aging of other phenolic compounds (Yu et al., 2014) and BB aerosols (Qi et al., 2019). Under N_2 -saturated conditions, oligomers with O:C ratios ≤ 0.6 were dominant in VL^* , while smaller molecules ($n_c \leq 8$) with higher O:C ratios (up to 0.8) were also observed for VL + AN. In contrast, more products with higher O:C ratios (≥ 0.6) were noted under air-saturated conditions for both VL^* and VL + AN. For experiments A5 to A8, H:C ratios were mostly around 1.0, and double bond equivalent (DBE) values were typically (58 % of the 50 most abundant products) > 7 , indicating that the products were mainly oxidized aromatic compounds (Xie et al., 2020). Compounds with H:C ≤ 1.0 and O:C ≤ 0.5 are common for aromatic species, while compounds with H:C ≥ 1.5 and O:C ≤ 0.5 are typical for more aliphatic species (Mazzoleni et al., 2012; Kourtchev et al., 2014; Jiang et al., 2021). In contrast, Loisel et al. (2021) reported mainly oxygenated aliphatic-like compounds from the direct irradiation of VL (0.1 mM), attributable to their use of ESI in the negative ion mode, which has higher sensitivity for detecting compounds such as carboxylic acids (Holčapek et al., 2010; Liigand et al., 2017) and the solid-phase extraction (SPE) procedure causing the loss of some oligomers (LeClair et al., 2012; Zhao et al., 2013; Bianco et al., 2019). Among experiments A5 to A8, VL + AN under air-saturated conditions (A7) had the highest normalized abundance of products and $\langle OS_c \rangle$, probably due to the combined influence of $^3VL^*$ and enhanced VL nitration in the presence of O_2 . Our measured $\langle OS_c \rangle$ for all experiments range from -0.28 to $+0.12$, while other studies on phenolic aqSOA formation reported $\langle OS_c \rangle$ ranging from -0.14 to $+0.47$ (Sun et al., 2010) and 0.04 to 0.74 (Yu et al., 2014). The $\langle OS_c \rangle$ in this study were likely lower estimates since we excluded contributions from ring-opening products, which may have higher OS_c values, as these products are not detectable in the positive ion mode. In brief, more oxidized aqSOA and higher normalized abundance of products, such as high O:C ratio oligomers and functionalized monomers, were noted under air-saturated conditions due to efficient VL oxidation by $^3VL^*$ in the presence of O_2 . Compared to N_2 -saturated conditions, the higher normalized abundance of N-containing products under air-saturated conditions for VL + AN (at pH 4) suggests a potential enhancement of VL nitration in the presence of O_2 .

Illumination of phenolic aromatic carbonyls with high molar absorptivities ($\epsilon_{\lambda_{max}}$; ~ 8 to $22 \times 10^3 \text{ M}^{-1} \text{ cm}^{-1}$) leads to an overall loss of light absorption, but increased absorbance at longer wavelengths ($> 350 \text{ nm}$), where the carbonyls did not initially absorb light (Smith et al., 2016). Figure 3a illustrates the changes in total absorbance from 350 to 550 nm of VL^* and VL + AN under N_2 - and air-saturated conditions. The absorption spectra of VL^* under air- and N_2 -saturated conditions (pH 4) at different time intervals are shown in Fig. S8. For both VL^* and VL + AN, evident absorbance enhancement was observed under air-saturated conditions, while the absorbance changes under N_2 -saturated conditions

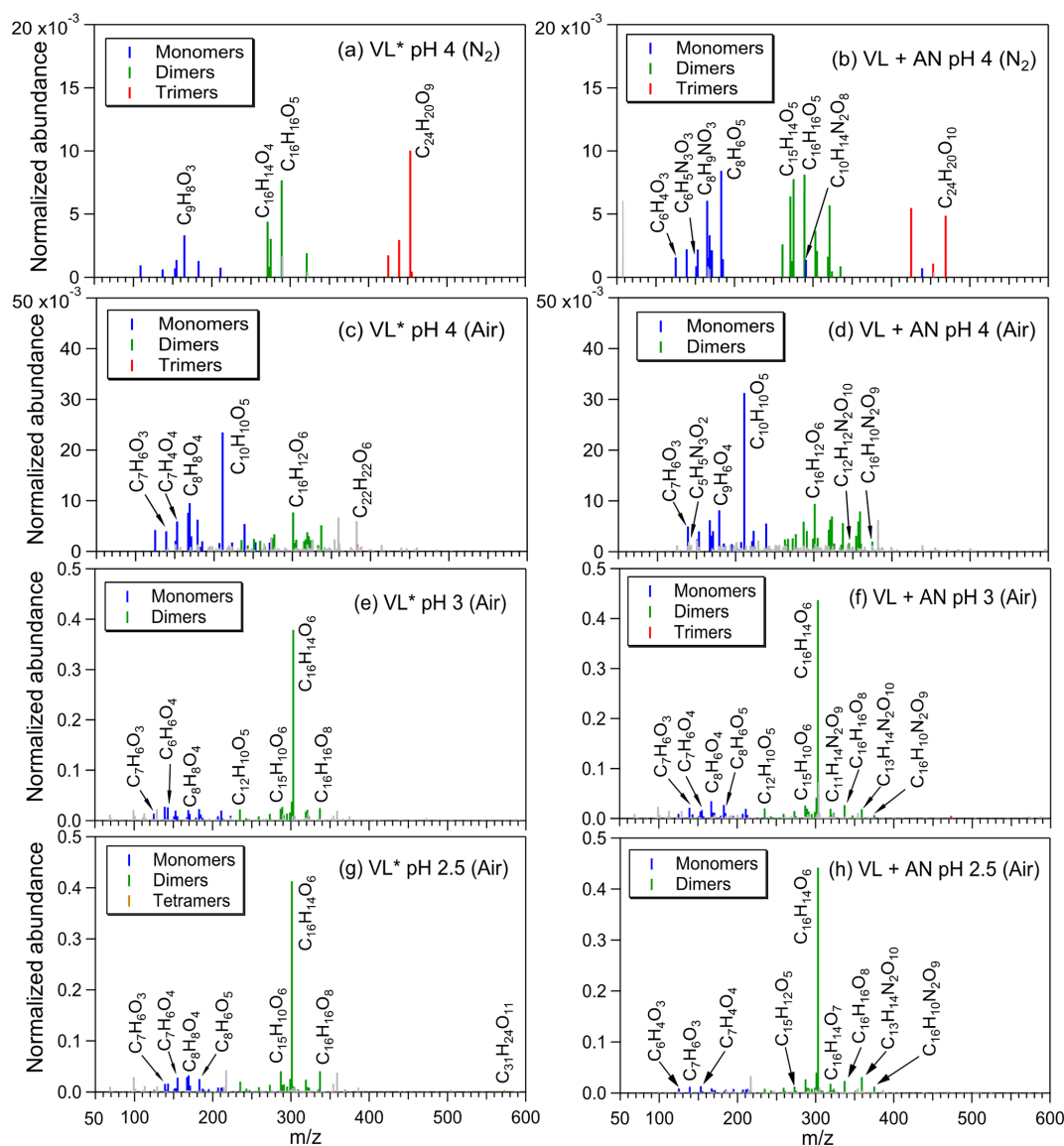


Figure 1. Reconstructed mass spectra of assigned peaks from (a) VL* pH 4 (N₂ saturated; A6), (b) VL + AN pH 4 (N₂ saturated; A8), (c) VL* pH 4 (air saturated; A5), (d) VL + AN pH 4 (air saturated; A7), (e) VL* pH 3 (air saturated; A3), (f) VL + AN pH 3 (air saturated; A4), (g) VL* pH 2.5 (air saturated; A1), and (h) VL + AN pH 2.5 (air saturated; A2) after 6 h of simulated sunlight irradiation. The normalized abundance of products was calculated using Eq. (2). The 50 most abundant products contributed more than half of the total normalized abundance of products, and they were identified as monomers (blue), dimers (green), trimers (red), and tetramers (orange). Gray peaks denote peaks with low abundance or an unassigned formula. Examples of high-intensity peaks were labeled with the corresponding neutral formulas. Note the different scales on the y axes.

were minimal, consistent with the VL decay trends. Dimers and functionalized products have been shown to contribute to chromophore formation for the aqueous photo-oxidation of guaiacyl acetone (another aromatic phenolic carbonyl) by ³DMB* (Jiang et al., 2021). Based on this, the higher normalized abundance of oligomers, which have large, conjugated π electron systems (Chang and Thompson, 2010), and hydroxylated products (Li et al., 2014; Zhao et al., 2015) observed under air-saturated conditions have contributed to the

absorbance enhancement. However, it is worth noting that the products detected may not have contributed significantly to the total products formed and, hence, may not be the primary contributors to the absorbance enhancement. As mentioned earlier, the major products detected in this study are probably those with high concentration or high ionization efficiency in the positive ESI mode. In other words, the absorbance enhancement may not necessarily correlate directly with the products detected.

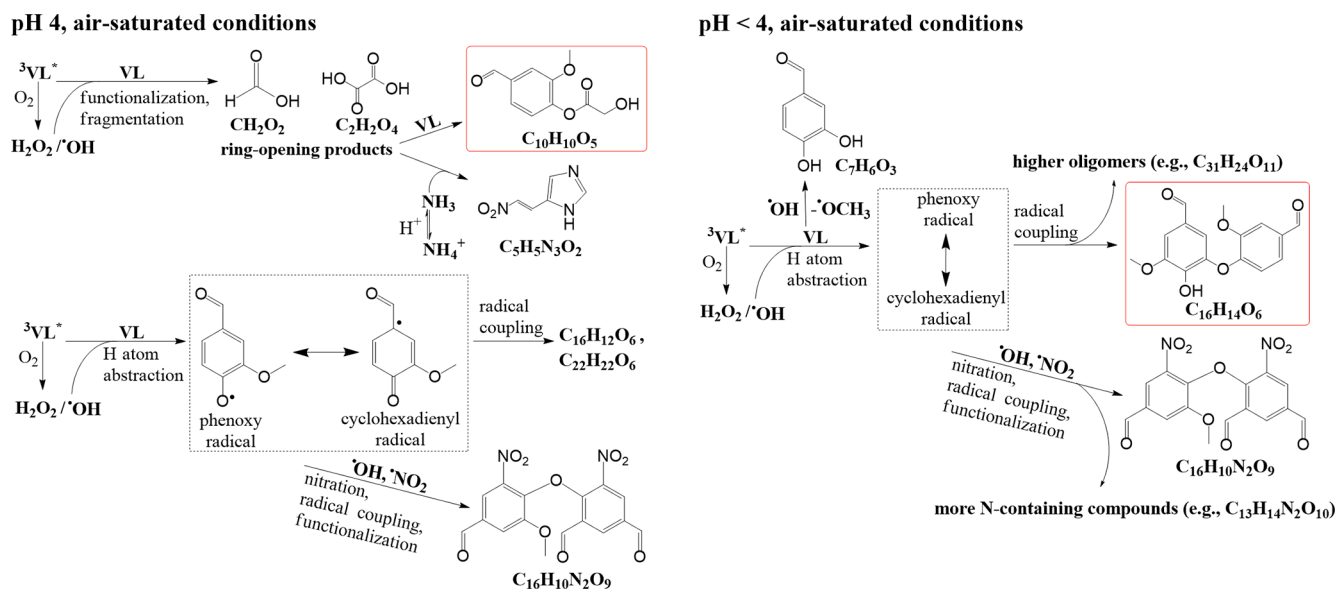


Figure 2. Potential aqSOA formation pathways via the direct photosensitized oxidation of VL in the absence (VL^*) and presence of ammonium nitrate ($\text{VL} + \text{AN}$) at pH 4 and pH < 4 under air-saturated conditions. Product structures were proposed based on the molecular formulas, double bond equivalent (DBE) values, and MS / MS fragmentation patterns. The structures presented were the major products detected using UHPLC-qToF-MS in positive ESI mode. The highlighted structures are the most abundant product for each condition.

Correlating speciated chromophores with absorbance changes may be useful in demonstrating how aqSOA influence the Earth's radiative balance and identifying chemical reactions that can affect the overall light absorption by aqSOA. This can be accomplished by using liquid chromatography (LC) coupled with photodiode array (PDA) detector and high-resolution mass spectrometry (HRMS; LC/PDA/HRMS platform; e.g., Lin et al., 2017; Jiang et al., 2021; Misovich et al., 2021). In our experiments, VL (and GUA) concentration measurements, product characterization, and absorbance measurements were performed using UHPLC-PDA, UHPLC-qToF-MS, and UV-Vis spectrophotometry, respectively. A similar approach is then possible using the current methods in this work by matching the retention time (RT) of the products detected using UHPLC-ToF-MS with that in the PDA. However, the concentration of the chromophores in this study is below the detection limit of the PDA, based on the lack of distinct PDA signals from the products. Absorbance increase at >350 nm has also been reported for the photosensitized oxidation of phenol and 4-phenoxyphenol (De Laurentiis et al., 2013a, b) and direct photolysis of tyrosine and 4-phenoxyphenol (Bianco et al., 2014) in which dimers have been identified as initial substrates. The continuous absorbance enhancement throughout 6 h of irradiation correlated with the observation of oligomers and nitrated compounds after irradiation. However, the increasing concentration of small organic acids (Fig. S5) throughout the experiments suggests that fragmentation, which results in the decomposition of initially formed oligomers and formation of smaller oxygenated

products (Huang et al., 2018), is important at longer irradiation times. Overall, these trends establish that compared to N_2 -saturated conditions, VL oxidation by $^3\text{VL}^*$ under air-saturated conditions (O_2 is present) enabled the efficient formation of light-absorbing compounds from both VL^* and $\text{VL} + \text{AN}$.

3.1.2 VL photo-oxidation under varying pH conditions

The reactions of $^3\text{C}^*$ (Smith et al., 2014, 2015, 2016), aromatic photolysis by nitrate (Machado and Boule, 1995; Dzenzel et al., 1999; Vione et al., 2005; Minero et al., 2007), and N(III)-mediated VL photo-oxidation (Pang et al., 2019a) have been demonstrated to be pH dependent. In this study, the effect of pH on the direct photosensitized oxidation of VL was investigated over the pH range of 2.5 to 4, which is within typical cloud pH values (2–7; Pye et al., 2020). The decay rate constants for both VL^* and $\text{VL} + \text{AN}$ increased by 1.6 and 1.4 times, respectively, as pH decreased from 4 to 2.5 (Table 2). These differences in the decay rate constants are small but statistically significant ($p < 0.05$). The pK_a for the $^3\text{VL}^*$ has been reported to be 4.0 (Smith et al., 2016). As there is a greater fraction of $^3\text{VL}^*$ that are protonated at pH 2.5 (0.96) than at pH 4 (0.50), it is possible that the pH dependence of the VL decay rate constants observed in this study is due to $^3\text{VL}^*$ being more reactive in its protonated form. Smith et al. (2016) also observed a pH dependence for the direct photodegradation of VL (0.005 mM; rate constants at $\text{pH} \leq 3$ are ~ 2 times lower than at $\text{pH} \geq 5$) which has been attributed to the sensitivity of the excimer of VL (i.e., the

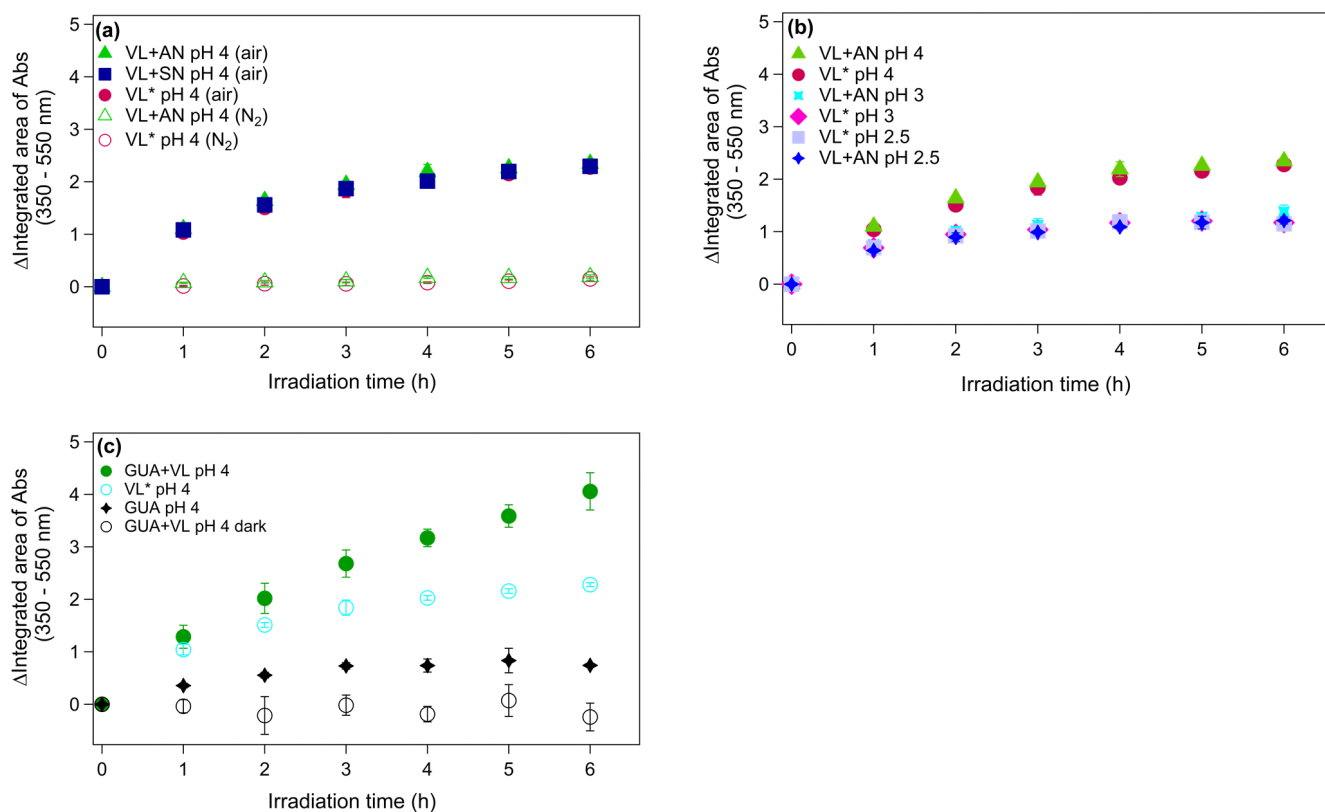


Figure 3. (a–c) Increase in light absorption under different experimental conditions for direct photosensitized oxidation of VL in the absence (VL^{*}) and presence of ammonium nitrate (VL + AN). (a) VL^{*} and VL + AN at pH 4 under N₂– (A6 and A8) and air-saturated (A5 and A7) conditions. Direct photosensitized oxidation of VL in the presence of sodium nitrate (VL + SN) at pH 4 under air-saturated conditions (A9). (b) Effect of pH on VL^{*} and VL + AN at pH 2.5 (A1 and A2), 3 (A3 and A4), and 4 (A5 and A7) under air-saturated conditions. (c) Increase in light absorption during direct GUA photodegradation (A13) and the oxidation of GUA via photosensitized reactions of VL (GUA + VL; A14) at pH 4 under air-saturated conditions after 6 h of simulated sunlight irradiation. Error bars represent 1 standard deviation; most error bars are smaller than the markers.

charge–transfer complex formed between an excited state VL molecule and a separate ground state VL molecule; Birks, 1973; Turro et al., 2010) to acid–base chemistry. The opposite trend observed in this study for 0.1 mM VL may be due to the reactivities of the protonated and neutral forms of ³VL^{*} being dependent on VL concentration (Smith et al., 2016). The quantum yield for direct VL photodegradation is higher at pH 5 than at pH 2 for 0.005 mM VL, but they are not statistically different for 0.03 mM VL (Smith et al., 2016). As pH decreases, the higher reactivity of ³VL^{*} and sensitivity of the excimer of VL to acid–base chemistry may have led to faster VL photo-oxidation. Similar to pH 4 experiments, comparable decay rate constants between VL^{*} and VL + AN were also noted at pH < 4, again suggesting the predominant role of ³VL^{*} chemistry compared to nitrate, likely due to the high VL concentration (0.1 mM) used in this study.

As pH decreased, the normalized abundance of products, particularly oligomers and functionalized monomers, was higher for both VL^{*} and VL + AN, consistent with ³VL^{*} potentially being more reactive in its protonated form. The

most abundant products observed were a substituted VL (C₁₀H₁₀O₅; no. 5 in Table S2) and VL dimer (C₁₆H₁₄O₆; no. 7 in Table S2) at pH 4 and pH < 4, respectively (Fig. 1c–h). Furthermore, a tetramer (C₃₁H₂₄O₁₁) was observed only in VL^{*} at pH 2.5. For VL + AN, the normalized abundance of N-containing compounds was also higher at lower pH (Table 2), likely due to increased [•]OH and [•]NO₂ formation, which may be caused by the dependence of N(III) (NO₂[−] + HONO) speciation on solution acidity (Pang et al., 2019a). At pH 3.3, half of N(III) exists as HONO (Fischer and Warneck, 1996; Pang et al., 2019a), which has a higher quantum yield for [•]OH formation than that of NO₂[−] in the near-UV region (Arakaki et al., 1999; Kim et al., 2014). Also, NO₂[−] / HONO can generate [•]NO₂ via oxidation by [•]OH (Reactions 4 and 10; Table 1; Pang et al., 2019a). At pH < 4, ³VL^{*} likely have higher reactivity, as suggested by the increased normalized abundance of oligomers (e.g., C₁₆H₁₄O₆; no. 7 in Table S2; C₃₁H₂₄O₁₁) and N-containing compounds (e.g., C₁₆H₁₀N₂O₉; no. 4 in Table S2; C₁₃H₁₄N₂O₁₀; Fig. 2). The most abundant product at pH < 4,

$C_{16}H_{14}O_6$ (no. 7 in Table S2) is likely a C–O coupled dimer. In previous studies on phenolic aqSOA formation, the generation of phenolic dimers has been proposed to occur via C–C or C–O coupling of phenoxy radicals (Sun et al., 2010; Yu et al., 2014; Huang et al., 2018; Chen et al., 2020; Misovich et al., 2021). Similarly, functionalized monomers, such as $C_7H_6O_3$ (demethylated VL; no. 8 in Table S2) and hydroxylated products (e.g., $C_8H_8O_4$; no. 9 in Table S2), also had increased normalized abundance for both VL* and VL + AN. The formation of $C_7H_6O_3$ (no. 8 in Table S2), which varies from the structure of VL by CH_2 , can be explained by $\cdot OH$ addition at the carbon containing the methoxy group, succeeded by the elimination of a methoxy radical ($\cdot OCH_3$; Yee et al., 2013). This reaction has also been postulated for the $\cdot OH$ oxidation of syringol (2,6-dimethoxyphenol; Yee et al., 2013) and transformation of DMB in a system composed of guaiacyl acetone and $^3DMB^*$ (Misovich et al., 2021). The potential imidazole derivative ($C_5H_5N_3O_2$; no. 6 in Table S2) was observed only at pH 4, following the pH dependence of ammonium speciation ($pK_a = 9.25$). Imidazole formation requires the nucleophilic attack of ammonia on the carbonyl group (Yu et al., 2011), and at pH 4, the concentration of dissolved ammonia in VL + AN was about 10 or 30 times higher than that at pH 3 or pH 2.5, respectively. For the pH values considered in this study, the O : C and H : C ratios in VL* and VL + AN had no significant differences (Figs. S7c–d and S9), but molecules with higher O : C ratios (>0.6) were more abundant at pH <4 . In addition, the $\langle OS_c \rangle$ at pH <4 for both VL* and VL + AN were higher than that at pH 4, consistent with higher $\langle OS_c \rangle$ observed at pH 5 compared to pH 7 for the $\cdot OH$ -mediated photo-oxidation of syringol (Sun et al., 2010). Essentially, the higher reactivity of $^3VL^*$ and predominance of HONO over nitrite at lower pH may have resulted in higher normalized abundance of products mainly composed of oligomers and functionalized monomers.

Higher absorbance enhancement for both VL* and VL + AN (Fig. 3b) was observed as pH increased. To determine whether the pH dependence is due to the acid–base chemistry of the products or of the reactions, the changes in the UV-Vis absorption spectra of the aqSOA formed from VL* at pH 4 and 2.5 were measured over a range of pH conditions from 1.5 to 10.5 (Fig. S10). For both cases, the intensity of absorption at longer wavelengths significantly increased as the pH of the solutions was raised. Moreover, the changes in the UV-Vis absorption spectra for the two solutions of varying pH are comparable, suggesting that the observed pH dependence is rooted in the acid–base chemistry of the reactions involving $^3VL^*$ or the excimer of VL (Smith et al., 2016), as discussed earlier.

3.1.3 Participation of ammonium in the direct photosensitized oxidation of VL in the presence of AN

Ammonium salts are an important constituent of atmospheric aerosols particles (Jimenez et al., 2009), and reactions between dicarbonyls (e.g., glyoxal) and ammonia or primary amines form BrC (De Haan et al., 2009, 2011; Nozière et al., 2009; Shapiro et al., 2009; Lee et al., 2013; Powelson et al., 2014; Gen et al., 2018; Mabato et al., 2019). Imidazole and imidazole derivatives are the major products of glyoxal and ammonium sulfate reactions at pH 4 (Galloway et al., 2009; Yu et al., 2011; Sedehi et al., 2013; Gen et al., 2018; Mabato et al., 2019). Here, we compared VL + AN and VL + SN at pH 4 under air-saturated conditions to confirm the participation of ammonium in the photosensitized oxidation of VL. The presence of ammonium did not appear to influence the kinetics of VL decay and light absorbance changes based on VL + AN and VL + SN, thus having no statistically significant difference ($p > 0.05$) with respect to VL decay rate constants (Table 2) and yielding comparable absorbance enhancement (Fig. 3a), respectively. However, it is important to note that this may not be the case for lower concentrations of VL. As previously stated, the reactions in this study were dominated by $^3VL^*$ chemistry, likely due to the higher molar absorptivity of VL than that of nitrate and the high VL concentration used. Similarly, the normalized abundance of products was comparable in both experiments (A7 and A9; Table 2), with $C_{10}H_{10}O_5$ (no. 5 in Table S2) as the most abundant product (Figs. 1d and S6a), but in VL + SN, there was a significant amount of a VL dimer ($C_{15}H_{12}O_8$; no. 10 in Table S2). The normalized abundance of N-containing compounds was also similar for VL + AN and VL + SN, but the detected N-containing compounds were distinct. Aside from the potential imidazole derivative ($C_5H_5N_3O_2$; no. 6 in Table S2), $C_8H_9NO_3$ (no. 3 in Table S2), possibly an aminophenol, was also observed from VL + AN – but only under N_2 -saturated conditions (Fig. 1b), probably due to further oxidation by $^3VL^*$. Relative to VL + AN, the products from VL + SN had higher O : C ratios (e.g., $C_7H_4N_2O_7$; no. 11 in Table S2), $\langle OS_c \rangle$, and $\langle OS_c \rangle$ values (Table 2). In summary, while the VL decay kinetics and absorbance enhancement for VL + AN and VL + SN were similar, the product analysis supports the participation of ammonium in the aqueous-phase reactions.

3.1.4 Distribution of potential BrC compounds

Figure S11 plots the DBE values vs. number of carbons (n_C ; Lin et al., 2018) for the 50 most abundant products from pH 4 experiments under air-saturated conditions, along with reference to DBE values corresponding to fullerene-like hydrocarbons (Lobodin et al., 2012), cata-condensed polycyclic aromatic hydrocarbons (PAHs; Siegmann and Sattler, 2000), and linear conjugated polyenes with a general for-

mula C_xH_{x+2} . As light absorption by BrC requires uninterrupted conjugation across a significant part of the molecular structure, compounds with DBE/ n_C ratios (shaded area in Fig. S11) greater than that of linear conjugated polyenes are potential BrC compounds (Lin et al., 2018). Based on this criterion and the observed absorbance enhancement at >350 nm (Fig. 3), the majority of the 50 most abundant products from pH 4 experiments under air-saturated conditions were potential BrC chromophores composed of monomers and oligomers up to tetramers. However, as ESI-detected compounds in BB organic aerosols has been reported to be mainly molecules with $n_C < 25$ (Lin et al., 2018), there may be higher oligomers that were not detected in our reaction systems.

3.2 Effect of reactants concentration and molar ratios on the direct photosensitized oxidation of VL in the aqueous phase

To examine the influence of VL and AN concentration and their molar ratios on the direct photosensitized oxidation of VL, we also characterized the reaction products from lower [VL] (0.01 mM VL^{*}; A10; Table 2), lower [VL] and equal molar ratio of VL / AN (0.01 mM VL + 0.01 mM AN; A11; Table 2), and lower [VL] and 1 : 100 molar ratio of VL / AN (0.01 mM VL + 1 mM AN; A12; Table 2) at pH 4. The normalized abundance of products from low [VL] experiments (A10–A12; Table 2) were up to 1.4 times higher than that of high [VL] experiments (A5 and A7; Table 2). Nevertheless, the major products for both low and high [VL] experiments were functionalized monomers (Figs. 1c and d and S12a–c) such as $C_8H_6O_4$ (no. 12 in Table S2) and $C_{10}H_{10}O_5$ (no. 5 in Table S2). For both VL^{*} and VL + AN, the contribution of <200 m/z to the normalized abundance of products was higher at low [VL] than at high [VL], while the opposite was observed for >300 m/z (Fig. S12d). This indicates that functionalization was favored at low [VL], as supported by the higher $\langle OS_c \rangle$, while oligomerization was the dominant pathway at high [VL], consistent with more oligomers or polymeric products reported from high phenols concentration (e.g., 0.1 to 3 mM; Li et al., 2014; Slikboer et al., 2015; Ye et al., 2019). As the formation mechanism of dimers and higher oligomers during aqueous-phase reactions of phenolic compounds involves the coupling of phenoxy radicals (Kobayashi and Higashimura, 2003; Sun et al., 2010), the enhanced oligomerization at high [VL] can be attributed to an increased concentration of phenoxy radicals (in resonance with a carbon-centered cyclohexadienyl radical) at high [VL], promoting radical–radical polymerization (Sun et al., 2010; Li et al., 2014). At low [VL], the contribution of <200 m/z to the normalized abundance of products was higher for 1 : 1 than 1 : 100 VL / AN molar ratio, suggesting the prevalence of functionalization for the former. In addition, 1 : 1 VL / AN (A11; Table 2) had higher $\langle OS_c \rangle$ than 1 : 100 VL / AN (A12; Table 2), indicating the forma-

tion of more oxidized products but fewer N-containing compounds compared to the latter. A possible explanation is that at 1 : 1 VL / AN, VL may compete with NO_2^- for *OH (from nitrate or nitrite photolysis; Reaction 4; Table 1) and indirectly reduce *NO_2 . Similarly, hydroxylation has been suggested to be a more important pathway for 1 : 1 VL / nitrite than in 1 : 10 VL / nitrite (Pang et al., 2019a). Fragmentation, which leads to the decomposition of previously formed oligomers and generation of small, oxygenated products such as organic acids (Huang et al., 2018) may also occur for the low [VL] experiments. However, its importance would likely be observed at longer irradiation times, similar to the high [VL] experiments.

3.3 Oxidation of guaiacol by photosensitized reactions of VL

The oxidation of phenols by $^3C^*$ has been mainly studied using non-phenolic aromatic carbonyls (Anastasio et al., 1997; Smith et al., 2014, 2015; Yu et al., 2014; Chen et al., 2020) and aromatic ketones (Canonica et al., 2000) as triplet precursors. Recently, $^3VL^*$ has been shown to oxidize syringol (Smith et al., 2016), a non-carbonyl phenol, although the reaction products remain unknown. In this section, we discussed the photo-oxidation of guaiacol (GUA), a non-carbonyl phenol that is also a lignocellulosic BB pollutant (Kroflíč et al., 2015), in the presence of VL (GUA + VL). The dark experiments did not show any substantial loss of VL or GUA (Fig. S3c). Due to its poor light absorption in the solar range, GUA is not an effective photosensitizer (Smith et al., 2014; Yu et al., 2014). Accordingly, direct GUA photodegradation resulted in minimal decay, which plateaued after ~ 3 h. In the presence of VL, the GUA decay rate constant was 2.2 times higher due to the oxidation of GUA by $^3VL^*$. The decay rate constant of VL in GUA + VL (A14; Table 2) was 3 times slower than that of VL^{*} (A5; Table 2), which may be due to competition between ground-state VL and GUA for reactions with $^3VL^*$ or the increased conversion of $^3VL^*$ back to the ground state through the oxidation of GUA (Anastasio et al., 1997; Smith et al., 2014).

For GUA experiments, the normalized abundance of products was calculated only for GUA + VL (2.2; Table 2) as the GUA signal from the UHPLC–qToF–MS in the positive ion mode was weak, which may introduce large uncertainties during normalization. Nonetheless, the number of products detected from these experiments (178 and 844 for direct GUA photodegradation and GUA + VL, respectively) corroborates the kinetics results. The major products (Fig. 4a) from direct GUA photodegradation were $C_{14}H_{14}O_4$ (no. 13 in Table S2), a typical GUA dimer, and $C_{21}H_{20}O_6$ (no. 14 in Table S2), a trimer which likely originated from photoinduced O–H bond breaking (Berto et al., 2016). In general, higher absolute signal intensities were noted for oligomers (e.g., $C_{14}H_{14}O_4$ and $C_{21}H_{20}O_6$; nos. 13 and 14 in Table S2, respectively) and hydroxylated products (e.g.,

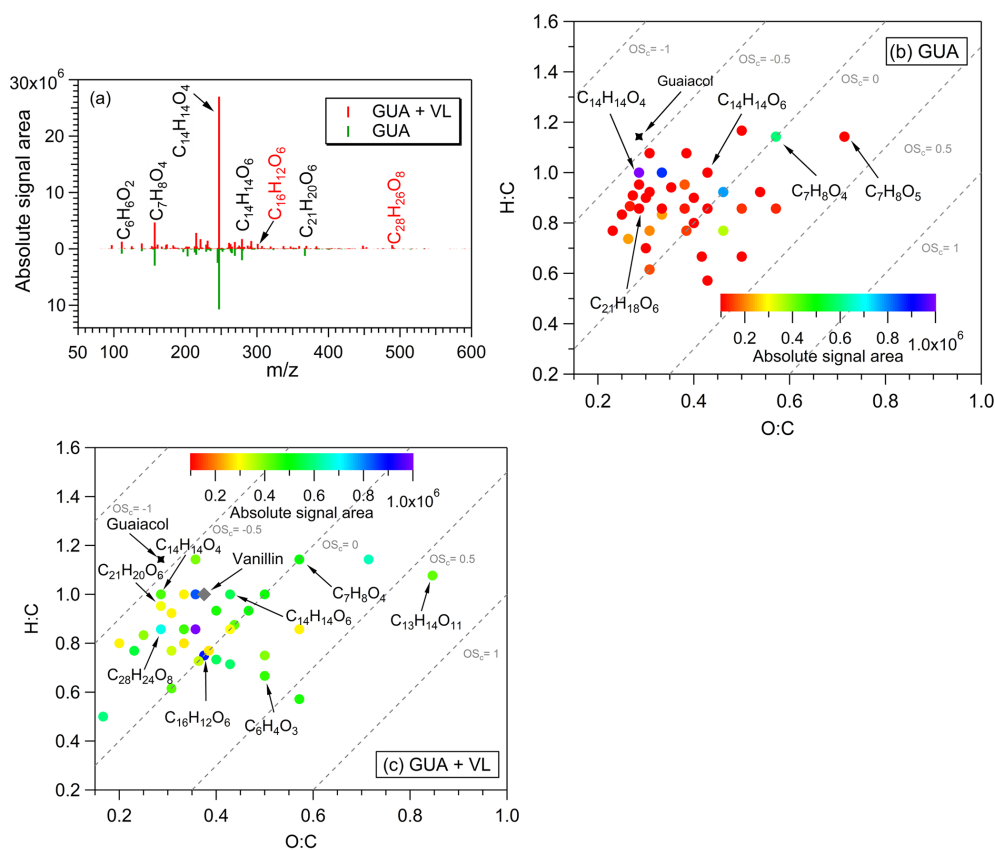


Figure 4. (a) Reconstructed mass spectra of assigned peaks from the direct GUA photodegradation (A13) and oxidation of GUA via photosensitized reactions of VL (GUA + VL; A14) at pH 4 under air-saturated conditions after 6 h of simulated sunlight irradiation. The y axis is the absolute signal area of the products. Examples of high-intensity peaks were labeled with the corresponding neutral formulas. The formulas in red text correspond to products observed only from GUA + VL. (b, c) Van Krevelen diagrams of the 50 most abundant products from the (b) direct photodegradation of GUA (A13) and (c) GUA + VL (A14) at pH 4 under air-saturated conditions after 6 h of simulated sunlight irradiation. The color bar denotes the absolute signal area. The gray dashed lines indicate the carbon oxidation state values (e.g., OS_c = −1, 0, and 1).

C₇H₈O₄) in GUA + VL, similar to those observed from GUA oxidation by ³DMB* or *OH (from H₂O₂ photolysis; Yu et al., 2014; Jiang et al., 2021). Also, a potential GUA tetramer (C₂₈H₂₆O₈; no. 15 in Table S2) was observed only in GUA + VL, consistent with more efficient oligomer formation from the triplet-mediated oxidation of phenols relative to direct photodegradation (Yu et al., 2014). The products from the direct GUA photodegradation and GUA + VL had mostly similar OS_c values (−0.5 to 0.5; Fig. 4b, c), falling into the criterion of biomass burning organic aerosol (BBOA) and semivolatile oxygenated organic aerosol (SV-OOA; Kroll et al., 2011). The corresponding absorbance changes for the GUA experiments (Fig. 3c) were consistent with the observed VL and GUA decay trends and detected products. While minimal absorbance changes, which also plateaued after ~ 3 h, were observed for direct GUA photodegradation, significant and continuous absorbance enhancement was noted for GUA + VL. Compared to direct GUA photodegradation, GUA oxidation by photosensitized

reactions of VL occurred rapidly and yielded higher absolute signal intensities for oligomers and hydroxylated products, which likely contributed to the pronounced absorbance enhancement.

4 Conclusions and atmospheric implications

In this study, the direct photosensitized oxidation of VL in the absence and presence of AN under atmospherically relevant cloud and fog conditions have been shown to generate aqSOA composed of oligomers, functionalized monomers, oxygenated ring-opening products, and nitrated compounds (from VL + AN). The oligomers from these reaction systems may be rather recalcitrant to fragmentation, based on their high normalized abundance, even at the longest irradiation time used in this study. Nonetheless, the increasing concentration of small organic acids over time implies that fragmentation becomes important at extended irradiation times. The reactions were observed to be influenced by O₂, pH, and re-

actants concentration and molar ratios. Our results suggest that O_2 could be required for the secondary steps in VL decay (e.g., the reaction of ketyl radical and O_2) via $^3VL^*$ to proceed. Compared to N_2 -saturated conditions, $^3VL^*$ -initiated reactions under air-saturated conditions (O_2 is present) proceeded rapidly, promoted the formation of more oxidized aqSOA, and generated products (e.g., oligomers, functionalized monomers, and N-containing compounds) with higher normalized abundance which exhibited stronger light absorption. For pH 4 experiments, the presence of both O_2 and nitrate resulted in the highest normalized abundance of products (including N-containing compounds) and $\langle OS_c \rangle$, which is attributed to O_2 promoting VL nitration. Nevertheless, further work on the effect of O_2 on the reactive intermediates involved in the reactions is necessary to elucidate the mechanisms of direct photosensitized oxidation of VL under air-saturated conditions. Additionally, the formation of oligomers from the direct photosensitized oxidation of VL was promoted at low pH (<4). Low VL concentration favored functionalization, while oligomerization prevailed at high VL concentration, consistent with past works (Li et al., 2014; Slikboer et al., 2015; Ye et al., 2019). Hydroxylation was observed to be important at equal molar ratios of VL and nitrate, likely due to VL competing with nitrite for $^{\bullet}OH$. Furthermore, the GUA experiments indicate that, in mixed biomass burning aerosols, triplet excited states of phenolic aromatic carbonyls can oxidize phenols, forming oligomers and hydroxylated products. Aromatic carbonyls and nitrophenols have been reported to be the most significant classes of BrC in cloud water heavily affected by biomass burning in the North China Plain (Desyaterik et al., 2013). Correspondingly, the most abundant products from our reaction systems (pH 4 and air-saturated solutions) are mainly potential BrC chromophores. These suggest that aqSOA generated in cloud and fog water from the oxidation of biomass burning aerosols via direct photosensitized reactions and nitrate photolysis products can impact aerosol optical properties and radiative forcing, particularly for areas where biomass burning is intensive.

Ammonium (and sodium) nitrate was not found to substantially affect the VL decay rate constants, likely due to the much higher molar absorptivity of VL than nitrate and high VL concentration used in this work. However, the presence of ammonium (and sodium) nitrate promoted functionalization and nitration, indicating the significance of nitrate photolysis for aqSOA formation from biomass-burning-derived compounds. This work demonstrates that nitration, which is an important process for producing light-absorbing organics or BrC (Jacobson, 1999; Kahnt et al., 2013; Mohr et al., 2013; Laskin et al., 2015; Teich et al., 2017; Li et al., 2020), can also affect the aqueous-phase processing of triplet-generating aromatics. In addition, a potential imidazole derivative observed from VL + AN at pH 4 reveals that ammonium participates in aqSOA formation from the photo-oxidation of phenolic aromatic carbonyls. This observation

also suggests that the photosensitized oxidation of phenolic aromatic carbonyls in the presence of AN could be a source of imidazoles in the aqueous phase. It is important to understand the source of imidazoles due to their possible effects on human health, their photosensitizing potential, and their effect on aerosol optical properties as BrC compounds (Teich et al., 2016).

A recent work (Ma et al., 2021) mimicking phenol oxidation by $^3DMB^*$ (a non-phenolic aromatic carbonyl) in more concentrated conditions of aerosol particles containing high AN concentration (0.5 M) increased the photodegradation rate constant for guaiacyl acetone (an aromatic phenolic carbonyl with high Henry's law constant; $1.2 \times 10^6 \text{ M atm}^{-1}$; McFall et al., 2020) by >20 times, which was ascribed to $^{\bullet}OH$ formation from nitrate photolysis (Brezonik and Fulkerson-Brekken, 1998; Chu and Anastasio, 2003). The same study also estimated that reactions of phenols with high Henry's law constants (10^6 to 10^9 M atm^{-1}) can be important for SOA formation in aerosol particles, with mechanisms mainly governed by $^3C^*$ and 1O_2 (Ma et al., 2021). Likewise, Zhou et al. (2019) reported that the direct photodegradation of acetosyringone was faster by about 6 times in the presence of 2 M NaClO_4 . However, the opposite was noted for the photodegradation of VL in sodium sulfate or sodium nitrate, which would occur slower (~ 2 times slower in 0.5 M sodium sulfate and ~ 10 times slower in 0.124 M sodium nitrate) in aerosol particles relative to dilute aqueous phase in clouds (Loisel et al., 2021), implying that the nature of inorganic ions may have an essential role in the photodegradation of organic compounds in the aqueous phase.

The concentrations of VL and nitrate can be significantly higher in aqueous aerosol particles than what we have used to mimic cloud and fog water. As a major component of aerosols, nitrate can have concentrations as high as sulfate (Huang et al., 2014). More studies should then explore the direct photosensitized oxidation of other biomass-burning-derived phenolic aromatic carbonyls, particularly those with high molar absorption coefficients. Based on our findings, the presence of nitrate should be considered for examining aqSOA formation from these reactions. The influences of reaction conditions should also be investigated to better understand the oxidation pathways. As aerosols comprise more complex mixtures of organic and inorganic compounds, it is worthwhile to explore the impacts of other potential aerosol constituents on aqSOA formation and photo-oxidation studies. This can also be beneficial for understanding the interplay among different reactions during photo-oxidation. Considering that biomass burning emissions are expected to increase continuously, further studies on these aqSOA formation pathways are strongly suggested.

Data availability. The data used in this publication are available to the community and can be accessed on request to the corresponding author.

Supplement. The supplement related to this article is available online at: <https://doi.org/10.5194/acp-22-273-2022-supplement>.

Author contributions. BRG designed and conducted the experiments. YL provided assistance with the measurements and helped to analyze experimental data. YJ provided assistance with the measurements. BRG, YL, and CKC wrote the paper. All co-authors contributed to the discussion of the draft versions of the paper.

Competing interests. The contact author has declared that neither they nor their co-authors have any competing interests.

Disclaimer. Publisher's note: Copernicus Publications remains neutral with regard to jurisdictional claims in published maps and institutional affiliations.

Acknowledgements. This work has been financially supported by the National Natural Science Foundation of China (grant nos. 41875142 and 42075100). Yong Jie Li acknowledges support from the Science and Technology Development Fund, Macau SAR (file no. 0019/2020/A1) and the Multi-Year Research grant (grant no. MYRG2018-00006-FST) from the University of Macau. Dan Dan Huang acknowledges support from the National Natural Science Foundation of China (grant no. 21806108). Xue Li acknowledges support from the Local Innovative and Research Teams Project of the Guangdong Pearl River Talents Program (grant no. 2019BT02Z546). Theodora Nah acknowledges support from the Hong Kong Research Grants Council (grant no. 21304919) and City University of Hong Kong (grant no. 9610409). Chun Ho Lam acknowledges support from the City University of Hong Kong (grant nos. 9610458 and 7005576).

Financial support. This research has been supported by the National Natural Science Foundation of China (grant nos. 41875142, 42075100, and 21806108), the Guangdong Provincial Pearl River Talents Program (grant no. 2019BT02Z546), the Research Grants Council, University Grants Committee (grant no. 21304919), the City University of Hong Kong (grant nos. 9610409, 9610458, and 7005576), the Science and Technology Development Fund (file no. 0019/2020/A1), and the Universidade de Macau, Research Services and Knowledge Transfer Office, University of Macau (grant no. MYRG2018-00006-FST).

Review statement. This paper was edited by Hang Su and reviewed by four anonymous referees.

References

Anastasio, C., Faust, B. C., and Rao, C. J.: Aromatic carbonyl compounds as aqueous-phase photochemical sources of hydrogen peroxide in acidic sulfate aerosols, fogs, and clouds.

1. Non-phenolic methoxybenzaldehydes and methoxyacetophenones with reductants (phenols), *Environ. Sci. Technol.*, 31, 218–232, <https://doi.org/10.1021/es960359g>, 1997.

Arakaki, T., Miyake, T., Hirakawa, T., and Sakugawa, H.: pH dependent photoformation of hydroxyl radical and absorbance of aqueous-phase N(III) (HNO_2 and NO_2^-), *Environ. Sci. Technol.*, 33, 2561–2565, <https://doi.org/10.1021/es980762i>, 1999.

Bateman, A. P., Laskin, J., Laskin, A., and Nizkorodov, S. A.: Applications of high-resolution electrospray ionization mass spectrometry to measurements of average oxygen to carbon ratios in secondary organic aerosols, *Environ. Sci. Technol.*, 46, 8315–8324, <https://doi.org/10.1021/es3017254>, 2012.

Benedict, K. B., McFall, A. S., and Anastasio, C.: Quantum yield of nitrite from the photolysis of aqueous nitrate above 300 nm, *Environ. Sci. Technol.*, 51, 4387–4395, <https://doi.org/10.1021/acs.est.6b06370>, 2017.

Berto, S., De Laurentiis, E., Tota, T., Chiavazza, E., Daniele, P. G., Minella, M., Isaia, M., Brigante, M., and Vione, D.: Properties of the humic-like material arising from the photo-transformation of L-tyrosine, *Sci. Total Environ.*, 545–546, 434–444, <https://doi.org/10.1016/j.scitotenv.2015.12.047>, 2016.

Bianco, A., Minella, M., De Laurentiis, E., Maurino, V., Minero, C., and Vione, D.: Photochemical generation of photoactive compounds with fulvic-like and humic-like fluorescence in aqueous solution, *Chemosphere*, 111, 529–536, <https://doi.org/10.1016/j.chemosphere.2014.04.035>, 2014.

Bianco, A., Riva, M., Baray, J.-L., Ribeiro, M., Chaumerliac, N., George, C., Bridoux, M., and Deguillaume, L.: Chemical characterization of cloud water collected at Puy de Dôme by FT-ICR MS reveals the presence of SOA components, *ACS Earth Space Chem.*, 3, 2076–2087, <https://doi.org/10.1021/acsearthspacechem.9b00153>, 2019.

Bianco, A., Passananti, M., Brigante, M., and Maillhot, G.: Photochemistry of the cloud aqueous phase: a review, *Molecules*, 25, 423, <https://doi.org/10.3390/molecules25020423>, 2020.

Birks, J. B.: *Organic Molecular Photophysics*, John Wiley & Sons, ISBN 9780471074151, 1973

Blando, J. D. and Turpin, B. J.: Secondary organic aerosol formation in cloud and fog droplets: a literature evaluation of plausibility, *Atmos. Environ.*, 34, 1623–1632, [https://doi.org/10.1016/S1352-2310\(99\)00392-1](https://doi.org/10.1016/S1352-2310(99)00392-1), 2000.

Bond, T. C., Streets, D. G., Yarber, K. F., Nelson, S. M., Woo, J.-H., and Klimont, Z.: A technology-based global inventory of black and organic carbon emissions from combustion, *J. Geophys. Res.*, 109, D14203, <https://doi.org/10.1029/2003JD003697>, 2004.

Brezonik, P. L. and Fulkerson-Brekken, J.: Nitrate-induced photolysis in natural waters: controls on concentrations of hydroxyl radical photo-intermediates by natural scavenging agents, *Environ. Sci. Technol.*, 32, 3004–3010, <https://doi.org/10.1021/es9802908>, 1998.

Canonica, S., Jans, U., Stemmler, K., and Hoigne, J.: Transformation kinetics of phenols in water: photosensitization by dissolved natural organic material and aromatic ketones, *Environ. Sci. Technol.*, 29, 1822–1831, <https://doi.org/10.1021/es00007a020>, 1995.

Canonica, S., Hellrung, B., and Wirz, J.: Oxidation of phenols by triplet aromatic ketones in aqueous solution, *J. Phys. Chem.*, 104, 1226–1232, <https://doi.org/10.1021/jp9930550>, 2000.

- Chang, J. L. and Thompson, J. E.: Characterization of colored products formed during irradiation of aqueous solutions containing H₂O₂ and phenolic compounds, *Atmos. Environ.*, 44, 541–551, <https://doi.org/10.1016/j.atmosenv.2009.10.042>, 2010.
- Chen, Y., Li, N., Li, X., Tao, Y., Luo, S., Zhao, Z., Ma, S., Huang, H., Chen, Y., Ye, Z., and Ge, X.: Secondary organic aerosol formation from ³C*-initiated oxidation of 4-ethylguaiaicol in atmospheric aqueous-phase, *Sci. Total Environ.*, 723, 137953, <https://doi.org/10.1016/j.scitotenv.2020.137953>, 2020.
- Chu, L. and Anastasio, C.: Quantum yields of hydroxyl radical and nitrogen dioxide from the photolysis of nitrate on ice, *J. Phys. Chem. A*, 107, 9594–9602, <https://doi.org/10.1021/jp0349132>, 2003.
- Collett Jr., J. L., Hoag, K. J., Sherman, D. E., Bator, A., and Richards, L. W.: Spatial and temporal variations in San Joaquin Valley fog chemistry, *Atmos. Environ.*, 33, 129–140, [https://doi.org/10.1016/S1352-2310\(98\)00136-8](https://doi.org/10.1016/S1352-2310(98)00136-8), 1998.
- De Haan, D. O., Corrigan, A. L., Tolbert, M. A., Jimenez, J. L., Wood, S. E., and Turley, J. J.: Secondary organic aerosol formation by self-reactions of methylglyoxal and glyoxal in evaporating droplets, *Environ. Sci. Technol.*, 43, 8184–8190, <https://doi.org/10.1021/es902152t>, 2009.
- De Haan, D. O., Hawkins, L. N., Kononenko, J. A., Turley, J. J., Corrigan, A. L., Tolbert, M. A., and Jimenez, J. L.: Formation of nitrogen-containing oligomers by methylglyoxal and amines in simulated evaporating cloud droplets, *Environ. Sci. Technol.*, 45, 984–991, <https://doi.org/10.1021/es102933x>, 2011.
- De Haan, D.O., Pajunaja, A., Hawkins, L. N., Welsh, H. G., Jimenez, N. G., De Loera, A., Zauscher, M., Andretta, A. D., Joyce, B. W., De Haan, A. C., Riva, M., Cui, T., Surratt, J. D., Cazaunau, M., Formenti, P., Gratien, A., Pangui, E., and Doussin, J-F: Methylamine's effects on methylglyoxal-containing aerosol: chemical, physical, and optical changes, *ACS Earth Space Chem.*, 3, 1706–1716, <https://doi.org/10.1021/acsearthspacechem.9b00103>, 2019.
- De Laurentiis, E., Socorro, J., Vione, D., Quivet, E., Brigante, M., Mailhot, G., Wortham, H., and Gligorovski, S.: Phototransformation of 4-phenoxyphenol sensitised by 4-carboxybenzophenone: Evidence of new photochemical pathways in the bulk aqueous phase and on the surface of aerosol deliquescent particles, *Atmos. Environ.*, 81, 569–578, <https://doi.org/10.1016/j.atmosenv.2013.09.036>, 2013a.
- De Laurentiis, E., Sur, B., Pazzi, M., Maurino, V., Minero, C., Mailhot, G., Brigante, M., and Vione, D.: Phenol transformation and dimerisation, photosensitised by the triplet state of 1-nitronaphthalene: a possible pathway to humic-like substances (HULIS) in atmospheric waters, *Atmos. Environ.*, 70, 318–327, <https://doi.org/10.1016/j.atmosenv.2013.01.014>, 2013b.
- Desyaterik, Y., Sun, Y., Shen, X., Lee, T., Wang, X., Wang, T., and Collett Jr., J. L.: Speciation of “brown” carbon in cloud water impacted by agricultural biomass burning in eastern China, *J. Geophys. Res.-Atmos.*, 118, 7389–7399, <https://doi.org/10.1002/jgrd.50561>, 2013.
- Du, Y., Fu, Q. S., Li, Y., and Su, Y.: Photodecomposition of 4-chlorophenol by reactive oxygen species in UV/air system, *J. Hazard. Mater.*, 186, 491–496, <https://doi.org/10.1016/j.jhazmat.2010.11.023>, 2011.
- Dzengel, J., Theurich, J., and Bahnemann, D. W.: Formation of nitroaromatic compounds in advanced oxidation processes: photolysis versus photocatalysis, *Environ. Sci. Technol.*, 33, 294–300, <https://doi.org/10.1021/es980358j>, 1999.
- Ervens, B., Turpin, B. J., and Weber, R. J.: Secondary organic aerosol formation in cloud droplets and aqueous particles (aq-SOA): a review of laboratory, field and model studies, *Atmos. Chem. Phys.*, 11, 11069–11102, <https://doi.org/10.5194/acp-11-11069-2011>, 2011.
- Fischer, M. and Warneck, P.: Photodecomposition of nitrite and undissociated nitrous acid in aqueous solution, *J. Phys. Chem.*, 100, 18749–18756, <https://doi.org/10.1021/jp961692+>, 1996.
- Fleming, L. T., Lin, P., Laskin, A., Laskin, J., Weltman, R., Edwards, R. D., Arora, N. K., Yadav, A., Meinardi, S., Blake, D. R., Pillarisetti, A., Smith, K. R., and Nizkorodov, S. A.: Molecular composition of particulate matter emissions from dung and brushwood burning household cookstoves in Haryana, India, *Atmos. Chem. Phys.*, 18, 2461–2480, <https://doi.org/10.5194/acp-18-2461-2018>, 2018.
- Foote, C. S.: Definition of type I and type II photosensitized oxidation, *Photochem. Photobiol.*, 54, 659, <https://doi.org/10.1111/j.1751-1097.1991.tb02071.x>, 1991.
- Galloway, M. M., Chhabra, P. S., Chan, A. W. H., Surratt, J. D., Flagan, R. C., Seinfeld, J. H., and Keutsch, F. N.: Glyoxal uptake on ammonium sulphate seed aerosol: reaction products and reversibility of uptake under dark and irradiated conditions, *Atmos. Chem. Phys.*, 9, 3331–3345, <https://doi.org/10.5194/acp-9-3331-2009>, 2009.
- Gelencsér, A., Hoffer, A., Kiss, G., Tombácz, E., Kurdi, R., and Bencze, L.: In-situ formation of light-absorbing organic matter in cloud water, *J. Atmos. Chem.*, 45, 25–33, <https://doi.org/10.1023/A:1024060428172>, 2003.
- Gen, M., Huang, D. D., and Chan, C. K.: Reactive uptake of glyoxal by ammonium-containing salt particles as a function of relative humidity, *Environ. Sci. Technol.*, 52, 6903–6911, <https://doi.org/10.1021/acs.est.8b00606>, 2018.
- Gen, M., Zhang, R., Huang, D. D., Li, Y., and Chan, C. K.: Heterogeneous SO₂ oxidation in sulfate formation by photolysis of particulate nitrate, *Environ. Sci. Technol. Lett.*, 6, 86–91, <https://doi.org/10.1021/acs.estlett.8b00681>, 2019a.
- Gen, M., Zhang, R., Huang, D. D., Li, Y., and Chan, C. K.: Heterogeneous oxidation of SO₂ in sulfate production during nitrate photolysis at 300nm: effect of pH, relative humidity, irradiation intensity, and the presence of organic compounds, *Environ. Sci. Technol.*, 53, 8757–8766, <https://doi.org/10.1021/acs.est.9b01623>, 2019b.
- George, C., Ammann, M., D’Anna, B., Donaldson, D. J., and Nizkorodov, S.A.: Heterogeneous photochemistry in the atmosphere, *Chem. Rev.*, 115, 4218–4258, <https://doi.org/10.1021/cr500648z>, 2015.
- George, C., Brüggemann, M., Hayeck, N., Tinel, L., and Donaldson, J.: Interfacial photochemistry: physical chemistry of gas-liquid interfaces, in: *Developments in Physical & Theoretical Chemistry*, edited by: Faust, J. A. and House, J. E., Elsevier, 435–457, <https://doi.org/10.1016/B978-0-12-813641-6.00014-5>, 2018.
- Gilardoni, S., Massoli, P., Paglione, M., Giulianelli, L., Carbone, C., Rinaldi, M., Decesari, S., Sandrini, S., Costabile, F., Gobbi, G. P., Pietrogrande, M. C., Visentin, M., Scotto, F., Fuzzi, S., and Facchini, M. C.: Direct observation of aqueous secondary organic aerosol from biomass-

- burning emissions, *P. Natl. Acad. Sci. USA*, 113, 10013–10018, <https://doi.org/10.1073/pnas.1602212113>, 2016.
- Giulianelli, L., Gilardoni, S., Tarozzi, L., Rinaldi, M., Decesari, S., Carbone, C., Facchini, M. C., and Fuzzi, S.: Fog occurrence and chemical composition in the Po valley over the last twenty years, *Atmos. Environ.*, 98, 394–401, <https://doi.org/10.1016/j.atmosenv.2014.08.080>, 2014.
- Goldstein, S. and Czapski, G.: Kinetics of nitric oxide autoxidation in aqueous solution in the absence and presence of various reductants. The nature of the oxidizing intermediates, *J. Am. Chem. Soc.*, 117, 12078–12084, <https://doi.org/10.1021/ja00154a007>, 1995.
- Grosjean, D.: Reactions of o-cresol and nitrocresol with nitrogen oxides (NO_x) in sunlight and with ozone–nitrogen dioxide mixtures in the dark, *Environ. Sci. Technol.*, 19, 968–974, <https://doi.org/10.1021/es00140a014>, 1985.
- Herrmann, H.: On the photolysis of simple anions and neutral molecules as sources of O^-/OH , SO_x^- and Cl in aqueous solution, *Phys. Chem. Chem. Phys.*, 9, 3935–3964, <https://doi.org/10.1039/B618565G>, 2007.
- Herrmann, H., Hoffmann, D., Schaefer, T., Brüner, P., and Tilgner, A.: Tropospheric aqueous-phase free-radical chemistry: radical sources, spectra, reaction kinetics and prediction tools, *Chem Phys Chem.*, 11, 3796–3822, <https://doi.org/10.1002/cphc.201000533>, 2010.
- Hoffer, A., Kiss, G., Blazsó, M., and Gelencsér, A.: Chemical characterization of humic-like substances (HULIS) formed from a lignin-type precursor in model cloud water, *Geophys. Res. Lett.*, 31, L06115, <https://doi.org/10.1029/2003GL018962>, 2004.
- Hoffmann, E. H., Tilgner, A., Wolke, R., Böge, O., Walter, A., and Herrmann, H.: Oxidation of substituted aromatic hydrocarbons in the tropospheric aqueous phase: kinetic mechanism development and modelling, *Phys. Chem. Chem. Phys.*, 20, 10960–10977, <https://doi.org/10.1039/C7CP08576A>, 2018.
- Holčapek, M., Jirásko, R., and Lísa, M.: Basic rules for the interpretation of atmospheric pressure ionization mass spectra of small molecules, *J. Chromatogr. A*, 1217, 3908–3921, <https://doi.org/10.1016/j.chroma.2010.02.049>, 2010.
- Huang, D. D., Zhang, Q., Cheung, H. H. Y., Yu, L., Zhou, S., Anastasio, C., Smith, J. D., and Chan, C. K.: Formation and evolution of aqSOA from aqueous-phase reactions of phenolic carbonyls: comparison between ammonium sulfate and ammonium nitrate solutions, *Environ. Sci. Technol.*, 52, 9215–9224, <https://doi.org/10.1021/acs.est.8b03441>, 2018.
- Huang, R.-J., Zhang, Y., Bozzetti, C., Ho, K.-F., Cao, J.-J., Han, Y., Daellenbach, K. R., Slowik, J. G., Platt, S. M., Canonaco, F., Zotter, P., Wolf, R., Pieber, S. M., Bruns, E. A., Crippa, M., Ciarelli, G., Piazzalunga, A., Schwikowski, M., Abbaszade, G., Schnelle-Kreis, J., Zimmermann, R., An, Z., Szidat, S., Baltensperger, U., El Haddad, I., and Prévôt, A. S. H.: High secondary aerosol contribution to particulate pollution during haze events in China, *Nature*, 514, 218–222, <https://doi.org/10.1038/nature13774>, 2014.
- Huang, X. H. H., Ip, H. S. S., and Yu, J. Z.: Secondary organic aerosol formation from ethylene in the urban atmosphere of Hong Kong: a multiphase chemical modeling study, *J. Geophys. Res.*, 116, D03206, <https://doi.org/10.1029/2010JD014121>, 2011.
- Jacobson, M. Z.: Isolating nitrated and aromatic aerosols and nitrated aromatic gases as sources of ultraviolet light absorption, *J. Geophys. Res.*, 104, 3527–3542, <https://doi.org/10.1029/1998JD100054>, 1999.
- Jiang, W., Misovich, M. V., Hettiyadura, A. P. S., Laskin, A., McFall, A. S., Anastasio, C., and Zhang, Q.: Photosensitized reactions of a phenolic carbonyl from wood combustion in the aqueous phase—chemical evolution and light absorption properties of aqSOA, *Environ. Sci. Technol.*, 55, 5199–5211, <https://doi.org/10.1021/acs.est.0c07581>, 2021.
- Jimenez, J. L., Canagaratna, M. R., Donahue, N. M., Prevot, A. S. H., Zhang, Q., Kroll, J. H., DeCarlo, P. F., Allan, J. D., Coe, H., Ng, N. L., Aiken, A. C., Docherty, K. S., Ulbrich, I. M., Grieshop, A. P., Robinson, A. L., Duplissy, J., Smith, J. D., Wilson, K. R., Lanz, V. A., Hueglin, C., Sun, Y. L., Tian, J., Laaksonen, A., Raatikainen, T., Rautiainen, J., Vaattovaara, P., Ehn, M., Kulmala, M., Tomlinson, J. M., Collins, D. R., Cubison, M. J., Dunlea, E. J., Huffman, J. A., Onasch, T. B., Alfarra, M. R., Williams, P. I., Bower, K., Kondo, Y., Schneider, J., Drewnick, F., Borrmann, S., Weimer, S., Demerjian, K., Salcedo, D., Cottrell, L., Griffin, R., Takami, A., Miyoshi, T., Hatakeyama, S., Shimono, A., Sun, J. Y., Zhang, Y. M., Dzepina, K., Kimmel, J. R., Sueper, D., Jayne, J. T., Herndon, S. C., Trimborn, A. M., Williams, L. R., Wood, E. C., Middlebrook, A. M., Kolb, C. E., Baltensperger, U., and Worsnop, D. R.: Evolution of organic aerosols in the atmosphere, *Science*, 326, 1525–1529, <https://doi.org/10.1126/science.1180353>, 2009.
- Kahnt, A., Behrouzi, S., Vermeylen, R., Shalamzari, M. S., Vercauteren, J., Roekens, E., Claeys, M., and Maenhaut, W.: One-year study of nitro-organic compounds and their relation to wood burning in PM_{10} aerosol from a rural site in Belgium, *Atmos. Environ.*, 81, 561–568, <https://doi.org/10.1016/j.atmosenv.2013.09.041>, 2013.
- Kaur, R. and Anastasio, C.: First measurements of organic triplet excited states in atmospheric waters, *Environ. Sci. Technol.*, 52, 5218–5226, <https://doi.org/10.1021/acs.est.7b06699>, 2018.
- Kaur, R., Labins, J. R., Helbock, S. S., Jiang, W., Bein, K. J., Zhang, Q., and Anastasio, C.: Photooxidants from brown carbon and other chromophores in illuminated particle extracts, *Atmos. Chem. Phys.*, 19, 6579–6594, <https://doi.org/10.5194/acp-19-6579-2019>, 2019.
- Kebarle, P.: A brief overview of the present status of the mechanisms involved in electrospray mass spectrometry, *J. Mass Spectrom.*, 35, 804–817, [https://doi.org/10.1002/1096-9888\(200007\)35:7<804::AID-JMS22>3.0.CO;2-Q](https://doi.org/10.1002/1096-9888(200007)35:7<804::AID-JMS22>3.0.CO;2-Q), 2000.
- Kim, D.-h., Lee, J., Ryu, J., Kim, K., and Choi, W.: Arsenite oxidation initiated by the UV photolysis of nitrite and nitrate, *Environ. Sci. Technol.*, 48, 4030–4037, <https://doi.org/10.1021/es500001q>, 2014.
- Kitanovski, Z., Čusak, A., Grgić, I., and Claeys, M.: Chemical characterization of the main products formed through aqueous-phase photolysis of guaiacol, *Atmos. Meas. Tech.*, 7, 2457–2470, <https://doi.org/10.5194/amt-7-2457-2014>, 2014.
- Klodt, A. L., Romonosky, D. E., Lin, P., Laskin, J., Laskin, A., and Nizkorodov, S. A.: Aqueous photochemistry of secondary organic aerosol of α -pinene and α -humulene in the presence of hydrogen peroxide or inorganic salts, *ACS Earth Space Chem.*, 3, 12, 2736–2746, <https://doi.org/10.1021/acsearthspacechem.9b00222>, 2019.

- Kobayashi, S. and Higashimura, H.: Oxidative polymerization of phenols revisited, *Prog. Polym. Sci.*, 28, 1015–1048, [https://doi.org/10.1016/S0079-6700\(03\)00014-5](https://doi.org/10.1016/S0079-6700(03)00014-5), 2003.
- Kourtchev, I., Fuller, S. J., Giorio, C., Healy, R. M., Wilson, E., O'Connor, I., Wenger, J. C., McLeod, M., Aalto, J., Ruuskanen, T. M., Maenhaut, W., Jones, R., Venables, D. S., Sodeau, J. R., Kulmala, M., and Kalberer, M.: Molecular composition of biogenic secondary organic aerosols using ultrahigh-resolution mass spectrometry: comparing laboratory and field studies, *Atmos. Chem. Phys.*, 14, 2155–2167, <https://doi.org/10.5194/acp-14-2155-2014>, 2014.
- Kroflić, A., Grilc, M., and Grgić, I.: Unraveling pathways of guaiacol nitration in atmospheric waters: nitrite, a source of reactive nitronium ion in the atmosphere, *Environ. Sci. Technol.*, 49, 9150–9158, <https://doi.org/10.1021/acs.est.5b01811>, 2015.
- Kroflić, A., Anders, J., Drventić, I., Mettke, P., Böge, O., Mutzel, A., Kleffmann, J., and Herrmann, H.: Guaiacol nitration in a simulated atmospheric aerosol with an emphasis on atmospheric nitrophenol formation mechanisms, *ACS Earth Space Chem.*, 5, 1083–1093, <https://doi.org/10.1021/acsearthspacechem.1c00014>, 2021.
- Kroll, J. H., Donahue, N. M., Jimenez, J. L., Kessler, S. H., Canagaratna, M. R., Wilson, K. R., Altieri, K. E., Mazzoleni, L. R., Wozniak, A. S., Bluhm, H., Mysak, E. R., Smith, J. D., Kolb, C. E., and Worsnop, D. R.: Carbon oxidation state as a metric for describing the chemistry of atmospheric organic aerosol, *Nat. Chem.*, 3, 133–139, <https://doi.org/10.1038/nchem.948>, 2011.
- Kruve, A., Kaupmees, K., Liigand, J., and Leito, I.: Negative electrospray ionization via deprotonation: predicting the ionization efficiency, *Anal. Chem.*, 86, 4822–4830, <https://doi.org/10.1021/ac404066v>, 2014.
- Laskin, A., Laskin, J., and Nizkorodov, S. A.: Chemistry of atmospheric brown carbon, *Chem. Rev.*, 115, 4335–4382, <https://doi.org/10.1021/cr5006167>, 2015.
- Laskin, J., Laskin, A., Nizkorodov, S. A., Roach, P., Eckert, P., Gilles, M. K., Wang, B., Lee, H. J., and Hu, Q.: Molecular selectivity of brown carbon chromophores, *Environ. Sci. Technol.*, 48, 12047–12055, <https://doi.org/10.1021/es503432r>, 2014.
- Lathioir, E. C., Leigh, W. J., and St. Pierre, M. J.: Geometrical effects on intramolecular quenching of aromatic ketone (π , π^*) triplets by remote phenolic hydrogen abstraction, *J. Am. Chem. Soc.*, 121, 11984–11992, <https://doi.org/10.1021/ja991207z>, 1999.
- LeClair, J. P., Collett, J. L., and Mazzoleni, L. R.: Fragmentation analysis of water-soluble atmospheric organic matter using ultrahigh-resolution FT-ICR mass spectrometry, *Environ. Sci. Technol.*, 46, 4312–4322, <https://doi.org/10.1021/es203509b>, 2012.
- Lee, A. K. Y., Herckes, P., Leitch, W. R., Macdonald, A. M., and Abbatt, J. P. D.: Aqueous OH oxidation of ambient organic aerosol and cloud water organics: Formation of highly oxidized products, *Geophys. Res. Lett.*, 38, L11805, <https://doi.org/10.1029/2011GL047439>, 2011.
- Lee, A. K. Y., Zhao, R., Li, R., Liggió, J., Li, S.-M., and Abbatt, J. P. D.: Formation of light absorbing organo-nitrogen species from evaporation of droplets containing glyoxal and ammonium sulfate, *Environ. Sci. Technol.*, 47, 12819–12826, <https://doi.org/10.1021/es402687w>, 2013.
- Lee, H. J., Aiona, P. K., Laskin, A., Laskin, J., and Nizkorodov, S. A.: Effect of solar radiation on the optical properties and molecular composition of laboratory proxies of atmospheric brown carbon, *Environ. Sci. Technol.*, 48, 10217–10226, <https://doi.org/10.1021/es502515r>, 2014.
- Lee, P. C. C. and Rodgers, M. A. J.: Laser flash photokinetic studies of Rose Bengal sensitized photodynamic interactions of nucleotides and DNA, *Photochem. Photobiol.*, 45, 79–86, <https://doi.org/10.1111/j.1751-1097.1987.tb08407.x>, 1987.
- Leito, I., Herodes, K., Huopola, M., Virro, K., Kunnas, A., Kruve, A., and Tanner, R.: Towards the electrospray ionization mass spectrometry ionization efficiency scale of organic compounds, *Rapid Commun. Mass Sp.*, 22, 379–384, <https://doi.org/10.1002/rcm.3371>, 2008.
- Li, X., Yang, Y., Liu, S., Zhao, Q., Wang, G., and Wang, Y.: Light absorption properties of brown carbon (BrC) in autumn and winter in Beijing: Composition, formation and contribution of nitrated aromatic compounds, *Atmos. Environ.*, 223, 117289, <https://doi.org/10.1016/j.atmosenv.2020.117289>, 2020.
- Li, P., Li, X., Yang, C., Wang, X., Chen, J., and Collett Jr., J. L.: Fog water chemistry in Shanghai, *Atmos. Environ.*, 45, 4034–4041, <https://doi.org/10.1016/j.atmosenv.2011.04.036>, 2011.
- Li, Y. J., Huang, D. D., Cheung, H. Y., Lee, A. K. Y., and Chan, C. K.: Aqueous-phase photochemical oxidation and direct photolysis of vanillin – a model compound of methoxy phenols from biomass burning, *Atmos. Chem. Phys.*, 14, 2871–2885, <https://doi.org/10.5194/acp-14-2871-2014>, 2014.
- Liang, Z., Zhang, R., Gen, M., Chu, Y., and Chan, C. K.: Nitrate photolysis in mixed sucrose–nitrate–sulfate particles at different relative humidities, *J. Phys. Chem. A*, 125, 3739–3747, <https://doi.org/10.1021/acs.jpca.1c00669>, 2021.
- Liigand, P., Kaupmees, K., Haav, K., Liigand, J., Leito, I., Girod, M., Antoine, R., and Kruve, A.: Think negative: finding the best electrospray ionization/MS mode for your analyte, *Anal. Chem.*, 89, 5665–5668, <https://doi.org/10.1021/acs.analchem.7b00096>, 2017.
- Lim, Y. B., Tan, Y., Perri, M. J., Seitzinger, S. P., and Turpin, B. J.: Aqueous chemistry and its role in secondary organic aerosol (SOA) formation, *Atmos. Chem. Phys.*, 10, 10521–10539, <https://doi.org/10.5194/acp-10-10521-2010>, 2010.
- Lin, P., Bluvshstein, N., Rudich, Y., Nizkorodov, S. A., Laskin, J., and Laskin, A.: Molecular chemistry of atmospheric brown carbon inferred from a nationwide biomass burning event, *Environ. Sci. Tech.*, 51, 11561–11570, <https://doi.org/10.1021/acs.est.7b02276>, 2017.
- Lin, P., Fleming, L. T., Nizkorodov, S. A., Laskin, J., and Laskin, A.: Comprehensive molecular characterization of atmospheric brown carbon by high resolution mass spectrometry with electrospray and atmospheric pressure photoionization, *Anal. Chem.*, 90, 12493–12502, <https://doi.org/10.1021/acs.analchem.8b02177>, 2018.
- Lin, P., Yu, J. Z., Engling, G., and Kalberer, M.: Organosulfates in humic-like substance fraction isolated from aerosols at seven locations in East Asia: a study by ultra-high-resolution mass spectrometry, *Environ. Sci. Technol.*, 46, 13118–13127, <https://doi.org/10.1021/es303570v>, 2012.
- Liu, C., Liu, J., Liu, Y., Chen, T., and He, H.: Secondary organic aerosol formation from the OH-initiated oxidation of guaiacol

- under different experimental conditions, *Atmos. Environ.*, 207, 30–37, <https://doi.org/10.1016/j.atmosenv.2019.03.021>, 2019.
- Lobodin, V. V., Marshall, A. G., and Hsu, C. S.: Compositional space boundaries for organic compounds, *Anal. Chem.*, 84, 3410–3416, <https://doi.org/10.1021/ac300244f>, 2012.
- Loisel, G., Mekic, M., Liu, S., Song, W., Jiang, B., Wang, Y., Deng, H., and Gligorovski, S.: Ionic strength effect on the formation of organonitrate compounds through photochemical degradation of vanillin in liquid water of aerosols, *Atmos. Environ.*, 246, 118140, <https://doi.org/10.1016/j.atmosenv.2020.118140>, 2021.
- Ma, L., Guzman, C., Niedek, C., Tran, T., Zhang, Q., and Anastasio, C.: Kinetics and mass yields of aqueous secondary organic aerosol from highly substituted phenols reacting with a triplet excited state, *Environ. Sci. Technol.*, 55, 5772–5781, <https://doi.org/10.1021/acs.est.1c00575>, 2021.
- Mabato, B. R. G., Gen, M., Chu, Y., and Chan, C. K.: Reactive uptake of glyoxal by methylammonium-containing salts as a function of relative humidity, *ACS Earth Space Chem.*, 3, 150–157, <https://doi.org/10.1021/acsearthspacechem.8b00154>, 2019.
- Machado, F. and Boule, P.: Photonitration and photonitrosation of phenolic derivatives induced in aqueous solution by excitation of nitrite and nitrate ions, *J. Photochem. Photobiol. A: Chem.*, 86, 73–80, [https://doi.org/10.1016/1010-6030\(94\)03946-R](https://doi.org/10.1016/1010-6030(94)03946-R), 1995.
- Mack, J. and Bolton, J. R.: Photochemistry of nitrite and nitrate in aqueous solution: a review, *J. Photochem. Photobiol. A*, 128, 1–13, [https://doi.org/10.1016/S1010-6030\(99\)00155-0](https://doi.org/10.1016/S1010-6030(99)00155-0), 1999.
- Mazzoleni, L. R., Saranjampour, P., Dalbec, M. M., Samburova, V., Hallar, A. G., Zielinska, B., Lowenthal, D. H., and Kohl, S.: Identification of water-soluble organic carbon in non-urban aerosols using ultrahigh-resolution FT-ICR mass spectrometry: organic anions, *Environ. Chem.*, 9, 285–297, <https://doi.org/10.1071/EN11167>, 2012.
- McFall, A. S., Johnson, A. W., and Anastasio, C.: Air–water partitioning of biomass-burning phenols and the effects of temperature and salinity, *Environ. Sci. Technol.*, 54, 3823–3830, <https://doi.org/10.1021/acs.est.9b06443>, 2020.
- McNally, A. M., Moody, E. C., and McNeill, K.: Kinetics and mechanism of the sensitized photodegradation of lignin model compounds, *Photochem. Photobiol. Sci.*, 4, 268–274, <https://doi.org/10.1039/B416956E>, 2005.
- Minella, M., Romeo, F., Vione, D., Maurino, V., and Minero, C.: Low to negligible photoactivity of lake-water matter in the size range from 0.1 to 5 μm , *Chemosphere*, 83, 1480–1485, <https://doi.org/10.1016/j.chemosphere.2011.02.093>, 2011.
- Minero, C., Bono, F., Rubertelli, F., Pavino, D., Maurino, V., Pelizzetti, E., and Vione, D.: On the effect of pH in aromatic photonitration upon nitrate photolysis, *Chemosphere*, 66, 650–656, <https://doi.org/10.1016/j.chemosphere.2006.07.082>, 2007.
- Misovich, M. V., Hettiyadura, A. P. S., Jiang, W., Zhang, Q., and Laskin, A.: Molecular-level study of the photo-oxidation of aqueous-phase guaiacyl acetone in the presence of $^3\text{C}^*$: formation of brown carbon products, *ACS Earth Space Chem.*, 5, 1983–1996, <https://doi.org/10.1021/acsearthspacechem.1c00103>, 2021.
- Mohr, C., Lopez-Hilfiker, F. D., Zotter, P., Prévôt, A. S. H., Xu, L., Ng, N. L., Herndon, S. C., Williams, L. R., Franklin, J. P., Zahniser, M. S., Worsnop, D. R., Knighton, W. B., Aiken, A. C., Gorkowski, K. J., Dubey, M. K., Allan, J. D., and Thornton, J. A.: Contribution of nitrated phenols to wood burn-
ing brown carbon light absorption in Detling, United Kingdom during winter time, *Environ. Sci. Technol.*, 47, 6316–6324, <https://doi.org/10.1021/es400683v>, 2013.
- Munger, J. W., Jacob, D. J., Waldman, J. M., and Hoffmann, M. R.: Fogwater chemistry in an urban atmosphere, *J. Geophys. Res.-Oceans*, 88, 5109–5121, <https://doi.org/10.1029/JC088iC09p05109>, 1983.
- Neumann, M. G., De Groot, R. A. M. C., and Machado, A. E. H.: Flash photolysis of lignin: Part 1. Deaerated solutions of dioxane-lignin, *Polym. Photochem.*, 7, 401–407, [https://doi.org/10.1016/0144-2880\(86\)90007-2](https://doi.org/10.1016/0144-2880(86)90007-2), 1986a.
- Neumann, M. G., De Groot, R. A. M. C., and Machado, A. E. H.: Flash photolysis of lignin: II. Oxidative photodegradation of dioxane-lignin, *Polym. Photochem.*, 7, 461–468, [https://doi.org/10.1016/0144-2880\(86\)90015-1](https://doi.org/10.1016/0144-2880(86)90015-1), 1986b.
- Ning, C., Gao, Y., Zhang, H., Yu, H., Wang, L., Geng, N., Cao, R., and Chen, J.: Molecular characterization of dissolved organic matters in winter atmospheric fine particulate matters ($\text{PM}_{2.5}$) from a coastal city of northeast China, *Sci. Total Environ.*, 689, 312–321, <https://doi.org/10.1016/j.scitotenv.2019.06.418>, 2019.
- Nolte, C. G., Schauer, J. J., Cass, G. R., and Simoneit, B. R. T.: Highly polar organic compounds present in wood smoke and in the ambient atmosphere, *Environ. Sci. Technol.*, 35, 1912–1919, <https://doi.org/10.1021/es001420r>, 2001.
- Nozière, B., Dziedzic, P., and Coirdova, A.: Products and kinetics of the liquid-phase reaction of glyoxal catalyzed by ammonium ions (NH_4^+), *J. Phys. Chem. A*, 113, 231–237, <https://doi.org/10.1021/jp8078293>, 2009.
- Nozière, B., Dziedzic, P., and Coirdova, A.: Inorganic ammonium salts and carbonate salts are efficient catalysts for aldol condensation in atmospheric aerosols, *Phys. Chem. Chem. Phys.*, 12, 3864–3872, <https://doi.org/10.1039/B924443C>, 2010.
- Nozière, B., Fache, F., Maxut, A., Fenet, B., Baudouin, A., Fine, L., and Ferronato, C.: The hydrolysis of epoxides catalyzed by inorganic ammonium salts in water: kinetic evidence for hydrogen bond catalysis, *Phys. Chem. Chem. Phys.*, 20, 1583–1590, <https://doi.org/10.1039/C7CP06790A>, 2018.
- Pang, H., Zhang, Q., Lu, X. H., Li, K., Chen, H., Chen, J., Yang, X., Ma, Y., Ma, J., and Huang, C.: Nitrite-mediated photooxidation of vanillin in the atmospheric aqueous phase, *Environ. Sci. Technol.*, 53, 14253–14263, <https://doi.org/10.1021/acs.est.9b03649>, 2019a.
- Pang, H., Zhang, Q., Wang, H., Cai, D., Ma, Y., Li, L., Li, K., Lu, X., Chen, H., Yang, X., and Chen, J.: Photochemical aging of guaiacol by Fe(III)-oxalate complexes in atmospheric aqueous phase, *Environ. Sci. Technol.*, 53, 127–136, <https://doi.org/10.1021/acs.est.8b04507>, 2019b.
- Perry, R. H., Cooks, R. G., and Noll, R. J.: Orbitrap mass spectrometry: instrumentation, ion motion and applications, *Mass Spectrom. Rev.*, 27, 661–699, <https://doi.org/10.1002/mas.20186>, 2008.
- Powelson, M. H., Espelien, B. M., Hawkins, L. N., Galloway, M. M., and De Haan, D. O.: Brown carbon formation by aqueous-phase carbonyl compound reactions with amines and ammonium sulfate, *Environ. Sci. Technol.*, 48, 985–993, <https://doi.org/10.1021/es4038325>, 2014.
- Pye, H. O. T., Nenes, A., Alexander, B., Ault, A. P., Barth, M. C., Clegg, S. L., Collett Jr., J. L., Fahey, K. M., Hennigan, C. J., Herrmann, H., Kanakidou, M., Kelly, J. T., Ku, I.-T., McNeill, V. F.,

- Riemer, N., Schaefer, T., Shi, G., Tilgner, A., Walker, J. T., Wang, T., Weber, R., Xing, J., Zaveri, R. A., and Zuend, A.: The acidity of atmospheric particles and clouds, *Atmos. Chem. Phys.*, 20, 4809–4888, <https://doi.org/10.5194/acp-20-4809-2020>, 2020.
- Qi, L., Chen, M., Stefenelli, G., Pospisilova, V., Tong, Y., Bertrand, A., Hueglin, C., Ge, X., Baltensperger, U., Prévôt, A. S. H., and Slowik, J. G.: Organic aerosol source apportionment in Zurich using an extractive electrospray ionization time-of-flight mass spectrometer (EESI-TOF-MS) – Part 2: Biomass burning influences in winter, *Atmos. Chem. Phys.*, 19, 8037–8062, <https://doi.org/10.5194/acp-19-8037-2019>, 2019.
- Rogge, W. F., Hildemann, L. M., Mazurek, M. A., and Cass, G. R.: Sources of fine organic aerosol. 9. Pine, oak, and synthetic log combustion in residential fireplaces, *Environ. Sci. Technol.*, 32, 13–22, <https://doi.org/10.1021/es960930b>, 1998.
- Romonosky, D. E., Li, Y., Shiraiwa, M., Laskin, A., Laskin, J., and Nizkorodov, S. A.: Aqueous photochemistry of secondary organic aerosol of α -Pinene and α -Humulene oxidized with ozone, hydroxyl radical, and nitrate radical, *J. Phys. Chem. A*, 121, 1298–1309, <https://doi.org/10.1021/acs.jpca.6b10900>, 2017.
- Scharko, N. K., Berke, A. E., and Raff, J. D.: Release of nitrous acid and nitrogen dioxide from nitrate photolysis in acidic aqueous solutions, *Environ. Sci. Technol.*, 48, 20, 11991–1200, <https://doi.org/10.1021/es503088x>, 2014.
- Schauer, J. J., Kleeman, M. J., Cass, G. R., and Simoneit, B. R. T.: Measurement of emissions from air pollution sources. 3. C₁–C₂₉ organic compounds from fireplace combustion of wood, *Environ. Sci. Technol.*, 35, 1716–1728, <https://doi.org/10.1021/es001331e>, 2001.
- Schmidt, A.-C., Herzs Schuh, R., Matysik, F.-M., and Engewald, W.: Investigation of the ionisation and fragmentation behaviour of different nitroaromatic compounds occurring as polar metabolites of explosives using electrospray ionisation tandem mass spectrometry, *Rapid Commun. Mass Sp.*, 20, 2293–2302, <https://doi.org/10.1002/rcm.2591>, 2006.
- Sedehi, N., Takano, H., Blasic, V. A., Sullivan, K. A., and De Haan, D. O.: Temperature- and pH-dependent aqueous-phase kinetics of the reactions of glyoxal and methylglyoxal with atmospheric amines and ammonium sulfate, *Atmos. Environ.*, 77, 656–663, <https://doi.org/10.1016/j.atmosenv.2013.05.070>, 2013.
- Shapiro, E. L., Szprengiel, J., Sareen, N., Jen, C. N., Giordano, M. R., and McNeill, V. F.: Light-absorbing secondary organic material formed by glyoxal in aqueous aerosol mimics, *Atmos. Chem. Phys.*, 9, 2289–2300, <https://doi.org/10.5194/acp-9-2289-2009>, 2009.
- Siegmann, K. and Sattler, K.: Formation mechanism for polycyclic aromatic hydrocarbons in methane flames, *J. Chem. Phys.*, 112, 698–709, <https://doi.org/10.1063/1.480648>, 2000.
- Slikboer, S., Grandy, L., Blair, S. L., Nizkorodov, S. A., Smith, R. W., and Al-Abadleh, H. A.: Formation of light absorbing soluble secondary organics and insoluble polymeric particles from the dark reaction of catechol and guaiacol with Fe(III), *Environ. Sci. Technol.*, 49, 7793–7801, <https://doi.org/10.1021/acs.est.5b01032>, 2015.
- Smith, J. D., Sio, V., Yu, L., Zhang, Q., and Anastasio, C.: Secondary organic aerosol production from aqueous reactions of atmospheric phenols with an organic triplet excited state, *Environ. Sci. Technol.*, 48, 1049–1057, <https://doi.org/10.1021/es4045715>, 2014.
- Smith, J. D., Kinney, H., and Anastasio, C.: Aqueous benzene-diols react with an organic triplet excited state and hydroxyl radical to form secondary organic aerosol, *Phys. Chem. Chem. Phys.*, 17, 10227–10237, <https://doi.org/10.1039/C4CP06095D>, 2015.
- Smith, J. D., Kinney, H., and Anastasio, C.: Phenolic carbonyls undergo rapid aqueous photodegradation to form low-volatility, light-absorbing products, *Atmos. Environ.*, 126, 36–44, <https://doi.org/10.1016/j.atmosenv.2015.11.035>, 2016.
- Song, J., Li, M., Jiang, B., Wei, S., Fan, X., and Peng, P.: Molecular characterization of water-soluble humic like substances in smoke particles emitted from combustion of biomass materials and coal using ultrahigh-resolution electrospray ionization Fourier transform ion cyclotron resonance mass spectrometry, *Environ. Sci. Technol.*, 52, 2575–2585, <https://doi.org/10.1021/acs.est.7b06126>, 2018.
- Sun, Y. L., Zhang, Q., Anastasio, C., and Sun, J.: Insights into secondary organic aerosol formed via aqueous-phase reactions of phenolic compounds based on high resolution mass spectrometry, *Atmos. Chem. Phys.*, 10, 4809–4822, <https://doi.org/10.5194/acp-10-4809-2010>, 2010.
- Teich, M., van Pinxteren, D., Kecorius, S., Wang, Z., and Herrmann, H.: First quantification of imidazoles in ambient aerosol particles: potential photosensitizers, brown carbon constituents, and hazardous components, *Environ. Sci. Technol.*, 50, 1166–1173, <https://doi.org/10.1021/acs.est.5b05474>, 2016.
- Teich, M., van Pinxteren, D., Wang, M., Kecorius, S., Wang, Z., Müller, T., Močnik, G., and Herrmann, H.: Contributions of nitrated aromatic compounds to the light absorption of water-soluble and particulate brown carbon in different atmospheric environments in Germany and China, *Atmos. Chem. Phys.*, 17, 1653–1672, <https://doi.org/10.5194/acp-17-1653-2017>, 2017.
- Tratnyek, P. G. and Hoigne, J.: Oxidation of substituted phenols in the environment: a QSAR analysis of rate constants for reaction with singlet oxygen, *Environ. Sci. Technol.*, 25, 1596–1604, <https://doi.org/10.1021/es00021a011>, 1991.
- Turro, N., Ramamurthy, V., and Scaiano, J. C.: *Modern Molecular Photochemistry*, University Science Books, ISBN 9781891389252, 2010.
- Vione, D., Albinet, A., Barsotti, F., Mekic, M., Jiang, B., Minero, C., Brigante, M., and Gligrovski, S.: Formation of substances with humic-like fluorescence properties, upon photoinduced oligomerization of typical phenolic compounds emitted by biomass burning, *Atmos. Environ.*, 206, 197–207, <https://doi.org/10.1016/j.atmosenv.2019.03.005>, 2019.
- Vione, D., Maurino, V., Minero, C., and Pelizzetti, E.: Phenol photolysis upon UV irradiation of nitrite in aqueous solution I: effects of oxygen and 2-propanol, *Chemosphere*, 45, 893–902, [https://doi.org/10.1016/S0045-6535\(01\)00035-2](https://doi.org/10.1016/S0045-6535(01)00035-2), 2001.
- Vione, D., Maurino, V., Minero, C., and Pelizzetti, E.: Reactions induced in natural waters by irradiation of nitrate and nitrite ions, in: *The Handbook of Environmental Chemistry*, vol. 2M, *Environmental Photochemistry Part II*, Springer, Berlin, Heidelberg, Germany, 221–253, <https://doi.org/10.1007/b138185>, 2005.
- Vione, D., Maurino, V., Minero, C., Pelizzetti, E., Harrison, M. A. J., Olariu, R., and Arsene, C.: Photochemical reactions in the tropospheric aqueous phase and on particulate matter, *Chem. Soc. Rev.*, 35, 441–453, <https://doi.org/10.1039/B510796M>, 2006.
- Volkamer, R., Ziemann, P. J., and Molina, M. J.: Secondary Organic Aerosol Formation from Acetylene (C₂H₂): seed ef-

- fect on SOA yields due to organic photochemistry in the aerosol aqueous phase, *Atmos. Chem. Phys.*, 9, 1907–1928, <https://doi.org/10.5194/acp-9-1907-2009>, 2009.
- Wang, K., Huang, R.-J., Brüggemann, M., Zhang, Y., Yang, L., Ni, H., Guo, J., Wang, M., Han, J., Bilde, M., Glasius, M., and Hoffmann, T.: Urban organic aerosol composition in eastern China differs from north to south: molecular insight from a liquid chromatography–mass spectrometry (Orbitrap) study, *Atmos. Chem. Phys.*, 21, 9089–9104, <https://doi.org/10.5194/acp-21-9089-2021>, 2021.
- Wang, X., Hayeck, N., Brüggemann, M., Yao, L., Chen, H., Zhang, C., Emmelin, C., Chen, J., George, C., and Wang, L.: Chemical characteristics of organic aerosols in Shanghai: a study by ultrahigh-performance liquid chromatography coupled with orbitrap mass spectrometry, *J. Geophys. Res.-Atmos.*, 122, 11703–11722, <https://doi.org/10.1002/2017JD026930>, 2017.
- Xiao, H.-W., Wu, J.-F., Luo, L., Liu, C., Xie, Y.-J., and Xiao, H.-Y.: Enhanced biomass burning as a source of aerosol ammonium over cities in Central China in autumn, *Environ. Pollut.*, 266, 115278, <https://doi.org/10.1016/j.envpol.2020.115278>, 2020.
- Xie, Q., Su, S., Chen, S., Xu, Y., Cao, D., Chen, J., Ren, L., Yue, S., Zhao, W., Sun, Y., Wang, Z., Tong, H., Su, H., Cheng, Y., Kawamura, K., Jiang, G., Liu, C.-Q., and Fu, P.: Molecular characterization of firework-related urban aerosols using Fourier transform ion cyclotron resonance mass spectrometry, *Atmos. Chem. Phys.*, 20, 6803–6820, <https://doi.org/10.5194/acp-20-6803-2020>, 2020.
- Yang, J., Au, W. C., Law, H., Lam, C. H., and Nah, T.: Formation and evolution of brown carbon during aqueous-phase nitrate-mediated photooxidation of guaiaicol and 5-nitroguaiacol, *Atmos. Environ.*, 254, 118401, <https://doi.org/10.1016/j.atmosenv.2021.118401>, 2021.
- Yaws, C. L.: Handbook of vapor pressure: Volume 3: Organic compounds C₈ to C₂₈, Gulf Professional Publishing, USA, ISBN 9780884151913, 1994.
- Ye, Z., Qu, Z., Ma, S., Luo, S., Chen, Y., Chen, H., Chen, Y., Zhao, Z., Chen, M., and Ge, X.: A comprehensive investigation of aqueous-phase photochemical oxidation of 4-ethylphenol, *Sci. Total Environ.*, 685, 976–985, <https://doi.org/10.1016/j.scitotenv.2019.06.276>, 2019.
- Yee, L. D., Kautzman, K. E., Loza, C. L., Schilling, K. A., Coggon, M. M., Chhabra, P. S., Chan, M. N., Chan, A. W. H., Hersey, S. P., Crouse, J. D., Wennberg, P. O., Flagan, R. C., and Seinfeld, J. H.: Secondary organic aerosol formation from biomass burning intermediates: phenol and methoxyphenols, *Atmos. Chem. Phys.*, 13, 8019–8043, <https://doi.org/10.5194/acp-13-8019-2013>, 2013.
- Yu, G., Bayer, A. R., Galloway, M. M., Korshavn, K. J., Fry, C. G., and Keutsch, F. N.: Glyoxal in aqueous ammonium sulfate solutions: products, kinetics and hydration effects, *Environ. Sci. Technol.*, 45, 6336–6342, <https://doi.org/10.1021/es200989n>, 2011.
- Yu, L., Smith, J., Laskin, A., Anastasio, C., Laskin, J., and Zhang, Q.: Chemical characterization of SOA formed from aqueous-phase reactions of phenols with the triplet excited state of carbonyl and hydroxyl radical, *Atmos. Chem. Phys.*, 14, 13801–13816, <https://doi.org/10.5194/acp-14-13801-2014>, 2014.
- Zhang, Q. and Anastasio, C.: Conversion of fogwater and aerosol organic nitrogen to ammonium, nitrate, and NO_x during exposure to simulated sunlight and ozone, *Environ. Sci. Technol.*, 37, 3522–3530, <https://doi.org/10.1021/es034114x>, 2003.
- Zhang, R., Gen, M., Huang, D. D., Li, Y., and Chan, C. K.: Enhanced sulfate production by nitrate photolysis in the presence of halide ions in atmospheric particles, *Environ. Sci. Technol.*, 54, 3831–3839, <https://doi.org/10.1021/acs.est.9b06445>, 2020.
- Zhang, R., Gen, M., Fu, T.-M., and Chan, C. K.: Production of formate via oxidation of glyoxal promoted by particulate nitrate photolysis, *Environ. Sci. Technol.*, 55, 5711–5720, <https://doi.org/10.1021/acs.est.0c08199>, 2021.
- Zhang, R., Gen, M., Liang, Z., Li, Y. J., and Chan, C. K.: Photochemical reactions of glyoxal during particulate ammonium nitrate photolysis: Brown carbon formation, enhanced glyoxal decay, and organic phase formation, *Environ. Sci. Technol.*, <https://doi.org/10.1021/acs.est.1c07211>, 2022.
- Zhao, R., Lee, A. K. Y., Huang, L., Li, X., Yang, F., and Abbatt, J. P. D.: Photochemical processing of aqueous atmospheric brown carbon, *Atmos. Chem. Phys.*, 15, 6087–6100, <https://doi.org/10.5194/acp-15-6087-2015>, 2015.
- Zhao, Y., Hallar, A. G., and Mazzoleni, L. R.: Atmospheric organic matter in clouds: exact masses and molecular formula identification using ultrahigh-resolution FT-ICR mass spectrometry, *Atmos. Chem. Phys.*, 13, 12343–12362, <https://doi.org/10.5194/acp-13-12343-2013>, 2013.
- Zhou, W., Mekic, M., Liu, J., Loisel, G., Jin, B., Vione, D., and Gligorovski, S.: Ionic strength effects on the photochemical degradation of acetosyringone in atmospheric deliquescent aerosol particles, *Atmos. Environ.*, 198, 83–88, <https://doi.org/10.1016/j.atmosenv.2018.10.047>, 2019.
- Zielinski, T., Bolzacchini, E., Cataldi, M., Ferrero, L., Graßl, S., Hansen, G., Mateos, D., Mazzola, M., Neuber, R., Pakszys, P., Posyniak, M., Ritter, C., Severi, M., Sobolewski, P., Traversi, R., and Velasco-Merino, C.: Study of chemical and optical properties of biomass burning aerosols during long-range transport events toward the Arctic in summer 2017, *Atmosphere*, 11, 84, <https://doi.org/10.3390/atmos11010084>, 2020.